Supporting Information

for

Wagner Meerwein-Type Rearrangements of Germapolysilanes - A Stable Ion Study

Lena Albers[a], *Mohammad Aghazadeh Meshgi*[c], *Judith Baumgartner*[b]*, *Christoph Marschner*[c]*, *Thomas Müller*[a*].

a. *Institut für Chemie der Carl von Ossietzky Universität Oldenburg, Carl von Ossietzky-Strasse 9 - 11, D-26129 Oldenburg, Federal Republic of Germany*

b. *Institut für Chemie der Karl Franzens Universität Graz, Stremayrgasse 9, 8010 Graz, Austria*

c. *Institut für Anorganische Chemie, Technische Universität Graz, Stremayrgasse 9, 8010 Graz, Austria*

Table of Contents.

Experimental part

All manipulations of air- and moisture-sensitive compounds were carried out under argon or nitrogen atmosphere using Schlenk techniques or a standard glove box (Braun Unilab). Glassware was dried in an oven at 120 °C and evacuated prior to use. The solvents tetrahydrofurane (THF), dimethoxyethane (DME), *n*-pentane, benzene and toluene were dried over sodium and distilled under nitrogen atmosphere. Chlorobenzene was dried over $CaCl_2$ and stored over molecular sieves. Deuterated benzene and toluene were stored over molecular sieves after drying over sodium. Dichlorodimethylgermane, chlorodimethylsilane, triethylsilane, tri-*iso*-propylsilane and trimethylchlorosilane were obtained from commercial suppliers and the silanes were dried over molecular sieves. Sodium methanolate was prepared by addition of sodium to an excess of *abs*. methanol. After all sodium was consumed the solvent was removed *in vacuo*. Triphenylmethyl tetrakis(pentafluorophenyl) borate **9** ($[Ph_3C][B(C_6F_5)_4]$) was prepared according to a modified literature procedure.[1] Tetrakis(trimethylsilyl)silane[2], tetrakis(trimethylsilyl)germane[3] **2**, tris(trimethylsilyl)silylpotassium[4], tris(trimethylsilyl)germylpotassium[5], tris(trimethylsilyl)silyltrimethylgermane[6] **1**, chloropentamethyldisilane[7] and trimethylsilane[8] were synthesized according to reported procedures. GC-MS spectra were performed on a Thermo Focus DSQ. NMR spectra were recorded on Bruker Avance 500, Bruker Avance III 500 and Varian Inova 300 spectrometers. ^{1}H NMR spectra were calibrated against the residual proton signal of the solvent as internal reference (benzene-d_6: $\delta^1H(C_6D_5H)$ = 7.20, toluene-d_8: $\delta^1H(CD_2H)$ = 2.08, chloroform-d_1: $\delta^1H(CHCl_3)$ = 7.24, chlorobenzene-d_5: $\delta^1H(C_6D_4HCl)$ = 7.14) and ^{13}C NMR spectra by using the central line of the solvent signal (benzene-d_6: $\delta^{13}C(C_6D_6)$ = 128.0, toluene-d_8: $\delta^{13}C(CD_3)$ = 20.4, chloroform-d_1: $\delta^{13}C(CDCl_3)$ = 77.0, chlorobenzene-d_5: $\delta^{13}C(C_6D_5Cl)$ = 134.2). ^{29}Si{^{1}H} NMR spectra were calibrated against an external standard ($^{29}Si(Me_2SiHCl)$ = 11.1 versus tetramethylsilane (TMS)). The ^{29}Si{^{1}H} NMR inverse gated spectra were recorded with a relaxation delay D1 = 10 s. Based on our experiences, at -20 °C this delay is long enough to allow a reliable integration of the peaks. The ^{29}Si{^{1}H} INEPT spectra were recorded with delays D3 = 0.0084 s and D4 = 0.0313 s. IR spectra were recorded on a Bruker Tensor 27 instrument. Analysis values for carbon show often too low values, which we attribute to the formation and incomplete combustion of silicon carbide, although vanadium pentoxide as combustion aid was used.

Dimethoxydimethylgermane[9] (17)

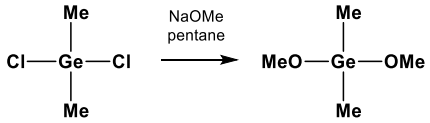

17

2.84 g (3.5 eq., 52.57 mmol) NaOMe was suspended in 40 mL pentane and 1.74 mL (15.00 mmol) dichlorodimethylgermane was slowly added with a syringe. The mixture was stirred overnight at room temperature. The excess of NaOMe and formed NaCl were separated from the solution by using a centrifuge

(20 min, 2000 rpm) and then the product-containing pentane solution was decanted using a Teflon tube. The salts were washed with 10 mL pentane and again centrifuged and decanted. The pentane solutions were combined and the product was separated from the solvent by fractionated distillation (bp.:118 °C at ambient pressure (1.45 g, 58 %). ^{1}H NMR (500.13 MHz, 297.9 K, C_6D_6, δ): 0.30 (s, 6H, $(CH_3)_2Ge$), 3.54 (s, 6H, $Ge(OCH_3)_2$). $^{13}C\{^{1}H\}$ NMR (125.77 MHz, 298.1K, C_6D_6, δ): -2.9 ($(CH_3)_2Ge$), 51.6 ($Ge(OCH_3)_2$). Mass required for $C_4H_{12}GeO_2$: 166.0. Mass found GC/MS: 164.9 (0.5) [M^+-H], 150.8 (100) [M^+-Me], 135.9 (72) [M^+-OMe], 120.9 (88) [M^+-OMe-Me], 104.9 (84) [M^+-OMe-2Me].

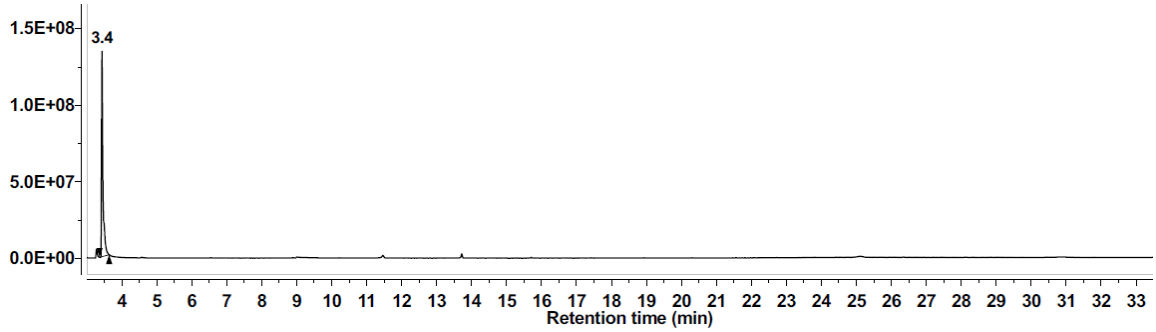

Figure S1. GC spectrum of dimethoxydimethylgermane (**17**)

Tris(trimethylsilyl)silyldimethylmethoxygermane (18)

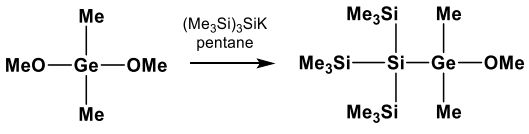

17 18

A solution of 4.50 mmol tris(trimethylsilyl)silylpotassium[4] in 40 mL pentane and a solution of 0.75 g (4.50 mmol) dimethoxydimethylgermane **17** in 10 mL pentane were cooled to 0 °C. The silyl potassium compound was added drop wise to the germane solution. The ice bath was allowed to warm to room temperature overnight. The reaction mixture was then hydrolyzed with 1 M hydrochloric acid. The organic layer was separated and dried over sodium sulfate. The solvent was removed under reduced pressure and the product was purified by Kugelrohr distillation (0.62 g, 36 %). Due to the use of hydrochloric acid about 14% of the corresponding germyl chloride was formed as a by-product, which was detected in the GC chromatograms and NMR spectra. ^{1}H NMR (499.87 MHz, 305.0 K, C_6D_6, δ ppm): 0.34 (s, 27H, $(CH_3)_3Si$), 0.60 (s, 6H, $(CH_3)_2Ge$), 3.54 (s, 3H, CH_3OGe). $^{13}C\{^{1}H\}$ NMR (125.69 MHz, 305.0 K, C_6D_6, δ ppm): 2.6 ($(CH_3)_3Si$), 4.1 ($(CH_3)_2Ge$), 52.6 (CH_3OGe). $^{29}Si\{^{1}H\}$ INEPT NMR (99.31 MHz, 305.0 K, C_6D_6, δ ppm): -124.6 ($(CH_3)_3Si)_3\underline{Si}$), -9.9 ($(CH_3)_3\underline{Si})_3Si$). Mass required for $C_{12}H_{36}GeOSi_4$: 382.1. Mass found GC/MS: 367.2 (1) [M^+-Me], 351.2 (0.5) [M^+-OMe], 278.0 (8) [M^+-$SiMe_3$-OMe], 205.1 (13) [M^+-2$SiMe_3$-OMe], 73.0 (100) [Me_3Si^+]. No satisfactory combustion analysis available due to contamination with the chloride side-product.

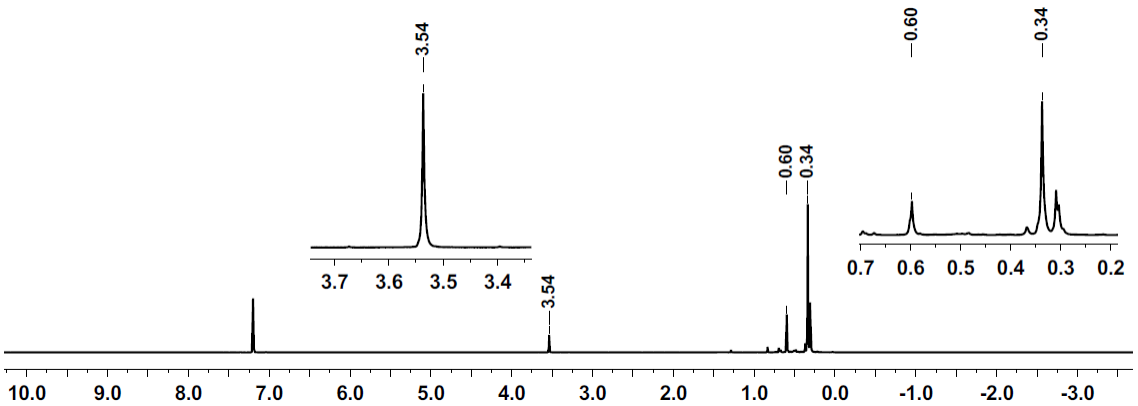

Figure S2a. ^{1}H NMR spectrum of a mixture of tris(trimethylsilyl)silyldimethylmethoxygermane (**18**) and tris(trimethylsilyl)silylchlorodimethylgermane in C_6D_6.

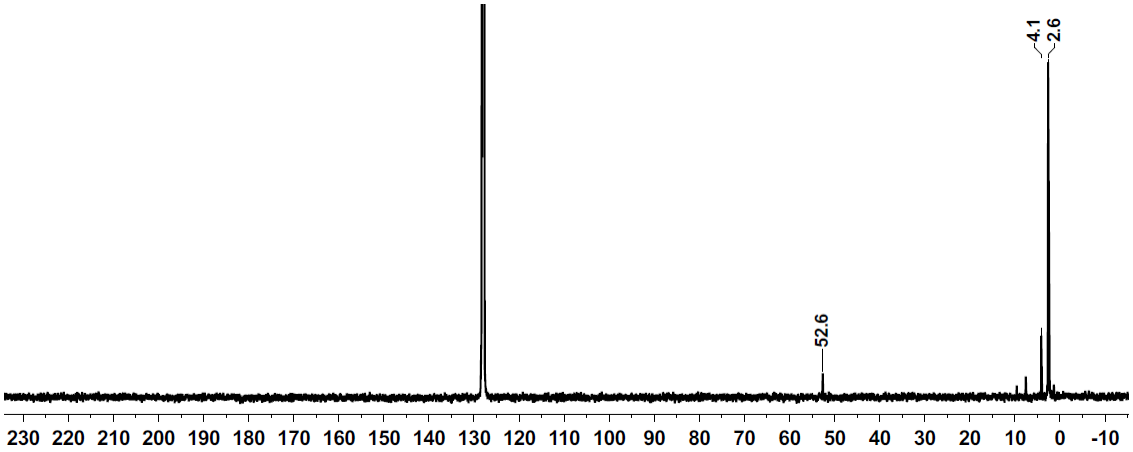

Figure S2b. $^{13}C\{^{1}H\}$ NMR spectrum of a mixture of tris(trimethylsilyl)silyldimethylmethoxygermane (**18**) and tris(trimethylsilyl)silylchlorodimethylgermane in C_6D_6.

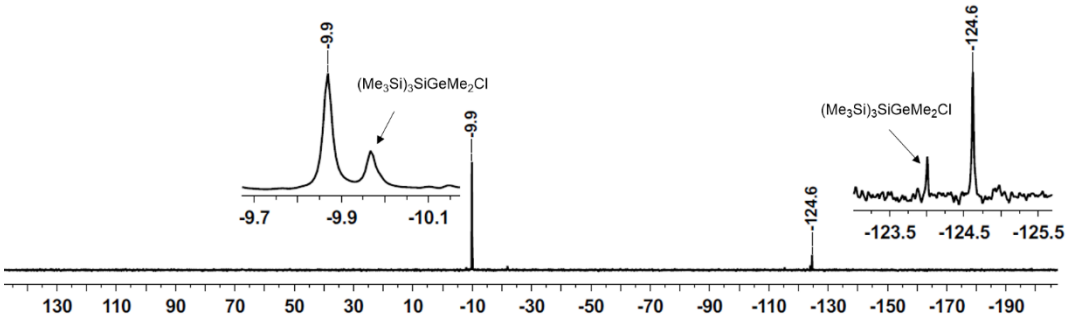

Figure S2c. $^{29}Si\{^{1}H\}$ NMR spectrum of a mixture of tris(trimethylsilyl)silyldimethylmethoxygermane (**18**) and tris(trimethylsilyl)silylchlorodimethylgermane in C_6D_6.

Tris(trimethylsilyl)silyldimethylgermane (14)

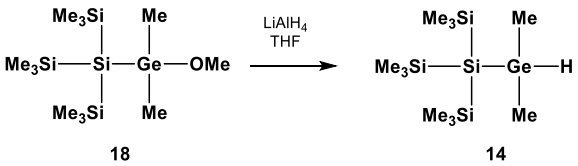

A solution of 0.62 g (1.62 mmol) tris(trimethylsilyl)silyldimethylmethoxygermane **18** in 30 mL THF and a suspension of 0.062 g (1.62 mmol) $LiAlH_4$ in 50 mL THF were cooled to 0 °C with an ice bath. The solution of silagermane **18** was added to the $LiAlH_4$ suspension and the reaction mixture was stirred for 20 min at 0 °C before it was allowed to warm to room temperature and stirred for another 20 min. The mixture was slowly added to ice cold 2 M sulfuric acid. The phases were separated and the aqueous phase was extracted two times with 50 mL diethyl ether. The combined organic phases were dried over sodium sulfate, filtered and the solvent was removed under reduced pressure. The product was crystallized from ethanol as a waxy, colorless solid (0.38 g, 1.09 mmol, 67 %). ^{1}H NMR (499.87 MHz, 305.0 K, C_6D_6, δ ppm): 0.30 (s, 27H, $(CH_3)_3Si$), 0.50 (d, $^{3}J_{H,H}$ = 4.2 Hz, 6H, $(CH_3)_2Ge$), 4.04 (sept, $^{3}J_{H,H}$ = 4.2 Hz, 1H, GeH). $^{13}C\{^{1}H\}$ NMR (125.69 MHz, 305.0 K, C_6D_6, δ ppm): -2.3 ($(CH_3)_2Ge$), 2.5 ($(CH_3)_3Si$). $^{29}Si\{^{1}H\}$ NMR (99.31 MHz, 305.0 K, C_6D_6, δ ppm): -128.3 ($(((CH_3)_3Si)_3\underline{Si}$), -9.4 ($(((CH_3)_3\underline{Si})_3Si$). Mass required for $C_{11}H_{34}GeSi_4$: 352.1. Mass found GC/MS: 351.1 (0.1) [M^+-H], 337.1 (0.6) [M^+-Me-H], 278.0 (30) [M^+-$SiMe_3$-H], 189.1 (13) [M^+-2$SiMe_3$-Me-H], 174.0 (4) [M^+-$SiMe_3$-$GeMe_2H$], 73.1 (100) [Me_3Si^+]. IR (ATR, neat): ν_{Ge-H} 1982 cm^{-1}, Anal. found/calcd. for $C_{11}H_{34}GeSi_4$: C 37.63/37.60, H 10.67/9.75.

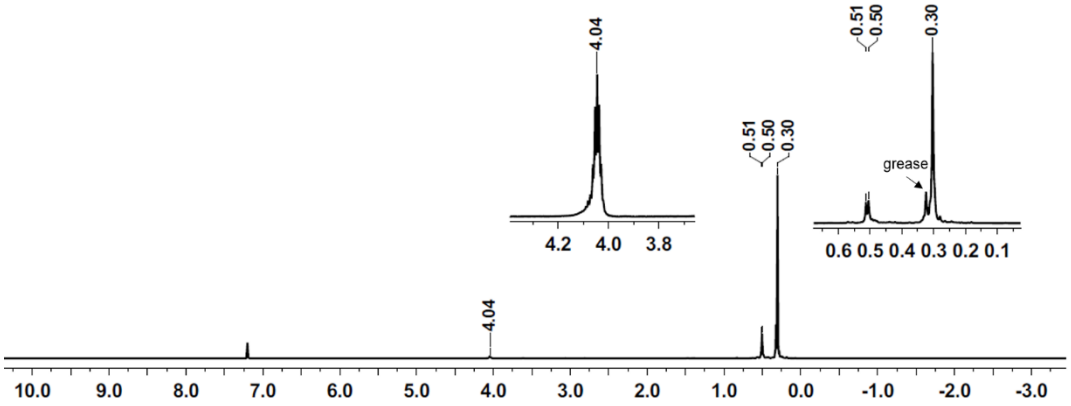

Figure S3a. ^{1}H NMR spectrum of tris(trimethylsilyl)silyldimethylgermane (**14**) in C_6D_6.

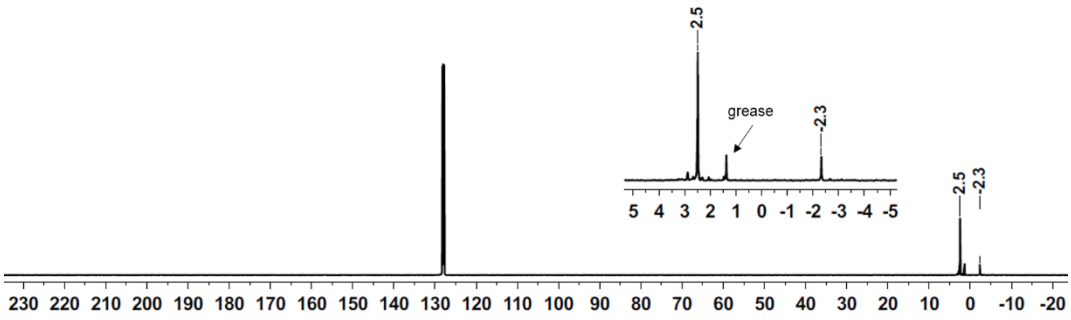

Figure S3b. $^{13}C\{^{1}H\}$ NMR spectrum of tris(trimethylsilyl)silyldimethylgermane (**14**) in C_6D_6.

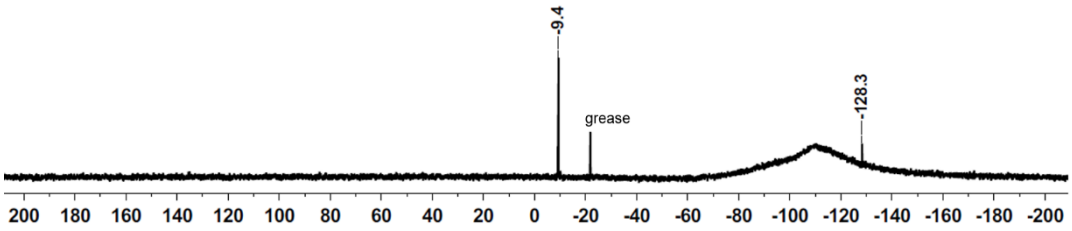

Figure S3c. $^{29}Si\{^{1}H\}$ NMR spectrum of tris(trimethylsilyl)silyldimethylgermane (**14**) in C_6D_6.

Tris(trimethylsilyl)germyldimethylsilane (15)[10]

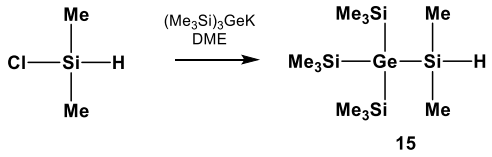

Solutions of 2.99 mmol tris(trimethylsilyl)germylpotassium[5] in 30 mL DME and of 0.6 mL (excess, 5.52 mmol) chlorodimethylsilane in 30 mL DME were cooled to 0 °C with an ice bath. The germylpotassium compound was slowly added to the chlorosilane solution during 1 h. The ice bath was allowed to warm to room temperature overnight. The reaction mixture was then hydrolyzed with 1 M sulfuric acid. The organic layer was separated and the aqueous phase was extracted with 10 mL diethyl ether. The combined organic phases were dried over sodium sulfate and the filtrate was concentrated to 5 mL under reduced pressure. The product crystallized by adding 2 mL acetonitrile as a colorless, waxy solid (0.847 g, 80.6 %). ^{1}H NMR (499.87 MHz, 305.0 K, $CDCl_3$, δ ppm)[10]: 0.22 (s, 27H, $(CH_3)_3Si$), 0.27 (d, $^{3}J_{H,H}$ = 4.2 Hz, 6H, $(CH_3)_2Si$), 4.12 (sept, $^{3}J_{H,H}$ = 4.2 Hz, 1H, SiH). $^{13}C\{^{1}H\}$ NMR (125.71 MHz, 305.0 K, $CDCl_3$, δ ppm): -1.4 ($(CH_3)_2Si$), 3.1 ($(CH_3)_3Si$). ^{29}Si INEPT NMR (99.31 MHz, 305.0 K, $CDCl_3$, δ ppm): -29.8 (dsept, $^{1}J_{Si,H}$ = 180.5 Hz, $^{2}J_{Si,H}$ = 7.0 Hz, SiH), -4.7 ($(CH_3)_3Si$). Mass required for $C_{11}H_{34}GeSi_4$: 352.1. Mass found GC/MS: m/z (%) = 351.1 (0.3) [M^+-H], 337.1 (2.5) [M^+-Me-H], 278.1 (64) [M^+-$SiMe_3$-H], 189.9 (22) [M^+-2$SiMe_3$-Me-H], 174.0 (2) [M^+-$SiMe_3$-$GeMe_2$H], 73.0 (100) [Me_3Si^+]. IR (ATR, neat): ν_{Si-H} 2085 cm^{-1}, Anal. found/calcd. for $C_{11}H_{34}GeSi_4$: C 36.31/37.60, H 9.98/9.75.

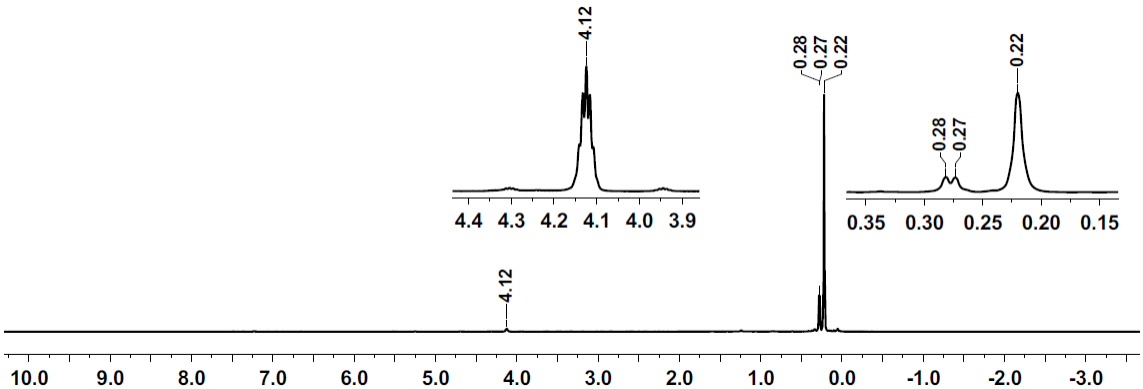

Figure S4a. ^{1}H NMR spectrum of tris(trimethylsilyl)germyldimethylsilane (**15**) in $CDCl_3$.

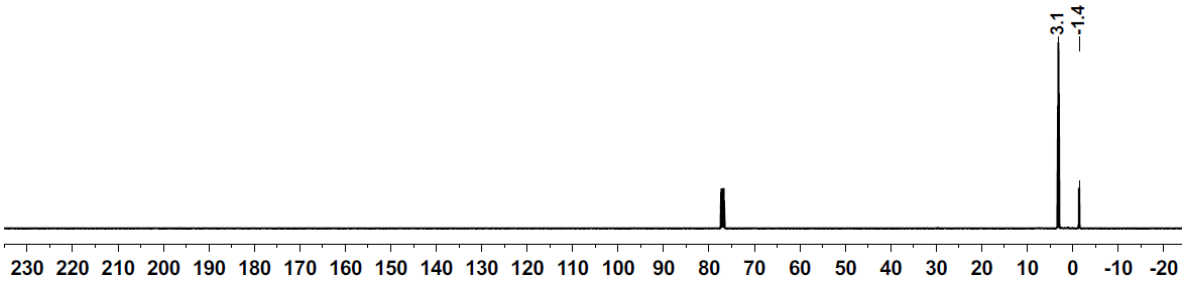

Figure S4b. $^{13}C\{^{1}H\}$ NMR spectrum of tris(trimethylsilyl)germyldimethylsilane (**15**) in $CDCl_3$.

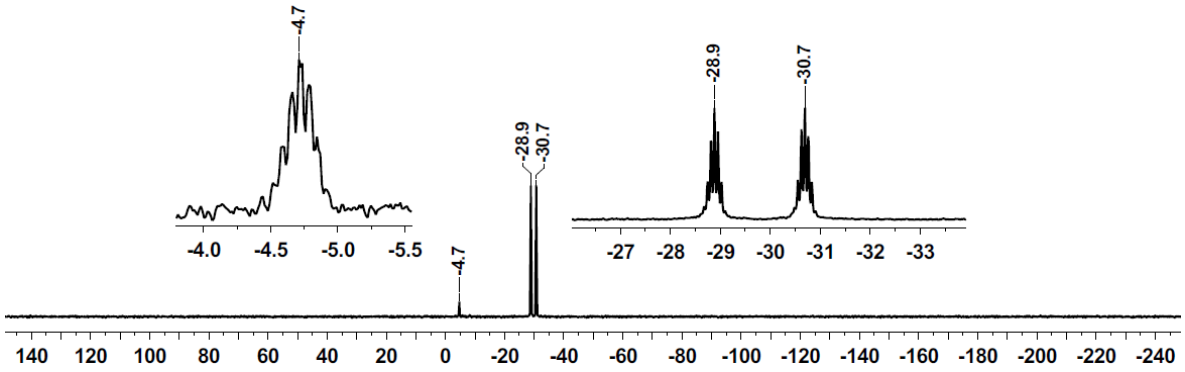

Figure S4c. ^{29}Si NMR spectrum of tris(trimethylsilyl)germyldimethylsilane (**15**) in $CDCl_3$.

Tris(trimethylsilyl)pentamethyldisilanylgermane (19)

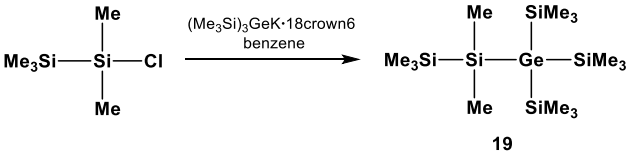

19

A solution of 1.37 mmol tris(trimethylsilyl)germylpotassium·18-crown-6[5] in 3 mL benzene was added drop wise to a solution of 0.25 g (1.51 mmol) chloropentamethyldisilane[7] in 3 mL benzene. After 5 h the solution mixture was quenched with 1M sulfuric acid and the phases were separated. The aqueous phase was extracted with pentane and the combined organic phases were dried over sodium sulfate, filtered and the sovent was removed under reduced pressure. The product was obtained as colorless crystals by crystallization from methanol/diethylether 1:2 (0.42 g, 73 %). ^{1}H NMR (299.94 MHz, 298.0 K, C_6D_6, δ ppm): 0.22 (s, 9H, $Si(CH_3)_2Si(C\underline{H}_3)_3$), 0.36 (s, 27H, $((C\underline{H}_3)_3Si)_3Ge$), 0.40 (s, 6H, $Si(C\underline{H}_3)_2Si(CH_3)_3$). $^{13}C\{^{1}H\}$ NMR (75.43 MHz, 298.0 K, C_6D_6, δ ppm): -0.8 ($Si(CH_3)_2Si(\underline{C}H_3)_3$), -0.4 ($Si(\underline{C}H_3)_2Si(CH_3)_3$), 4.0 ($(((\underline{C}H_3)_3Si)_3Ge$). $^{29}Si\{^{1}H\}$ INEPT NMR (59.59 MHz, 295.0 K, C_6D_6, δ ppm): -34.0 ($\underline{Si}(CH_3)_2Si(CH_3)_3$), -15.5 ($Si(CH_3)_2\underline{Si}(CH_3)_3$), -5.2 ($((CH_3)_3Si)_2Ge$). Mass required for $C_{14}H_{42}GeSi_5$: 424.1. Mass found GC/MS: m/z (%) = 424 (1) [M^+]; 408 (1) [M^+-Me-H]; 351 (3) [M^+-$SiMe_3$]; 278 (10) [M^+-2$SiMe_3$]; 259 (1) [$GeSi_3C_7H_{17}^+$]; 243 (1) [$GeSi_3C_6H_{13}^+$]; 219 (3) [$GeSi_2C_6H_{17}^+$]; 203 (11) [M^+-3$SiMe_3$-2H]; 187(8)[M^+-3$SiMe_3$-Me-4H]; 147 (7) [$GeSiMe_3^+$]; 131 (35) [$SiMe_3SiMe_2^+$]; 73 (100) [$SiMe_3^+$]. Anal. found/calcd. for $C_{14}H_{42}GeSi_5$ C 39.33/39.70, H 9.50/9.99.

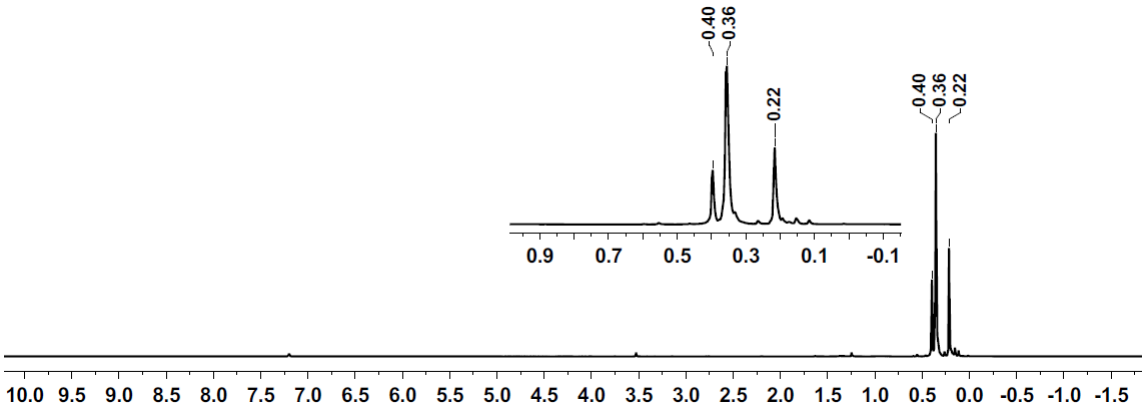

Figure S5a. ^{1}H NMR spectrum of tris(trimethylsilyl)pentamethyldisilanylgermane (**19**) in C_6D_6.

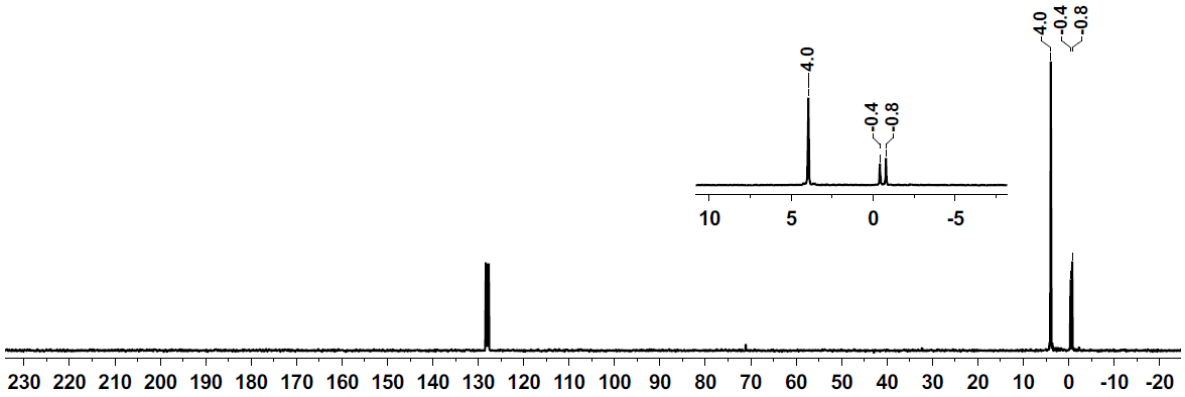

Figure S5b. ^{13}C{^{1}H} NMR spectrum of tris(trimethylsilyl)pentamethyldisilanylgermane (**19**) in C_6D_6.

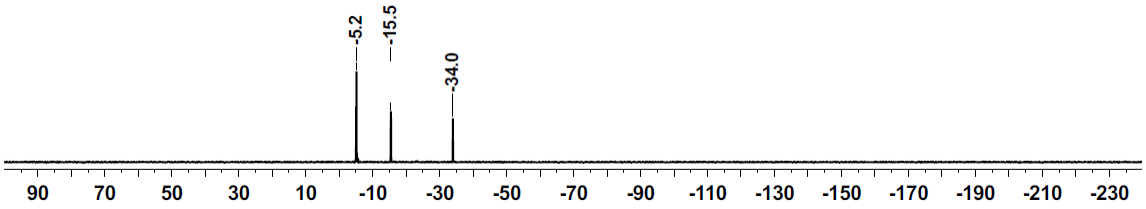

Figure S5c. ^{29}Si{^{1}H} INEPT NMR spectrum of tris(trimethylsilyl)pentamethyldisilanylgermane (**19**) in C_6D_6.

Bis(trimethylsilyl)pentamethyldisilanylgermane (16)

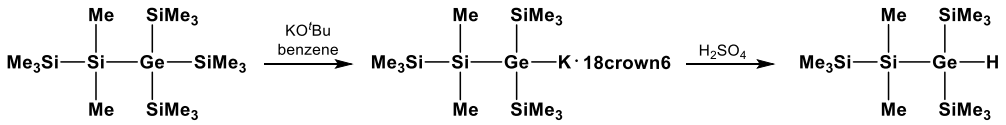

19 **20** **16**

A mixture of 0.21 g (0.49 mmol) germapolysilane **19**, 0.062 g (0.51 mmol) KO^{t}Bu and 0.134 g (0.51 mmol) 18-crown-6 ether was dissolved in 2 mL benzene. After the complete formation of the germylpotassium compound **20** was confirmed by NMR spectroscopy, the solution was added to a stirred mixture of 10 mL degassed diethyl ether and 20 mL degassed 2M sulfuric acid cooled with an ice bath. The phases were separated,

the aqueous phase was extracted with degassed diethyl ether and the combined organic phases dried over sodium sulfate. The solvents were removed under reduced pressure and the product was obtained as a colorless oil (0.15 g, 91 %) The germane is sensible to oxygen and should be stored under argon at -20 °C.

Bis(trimethylsilyl)pentamethyldisilanygermylpotassium (20)

^{1}H NMR (299.94 MHz, 298.0 K, C_6D_6, δ ppm): 0.39 (s, 9H $(Si(CH_3)_2)Si(C\underline{H}_3)_3$), 0.59 (s, 18H $((C\underline{H}_3)_3Si)_2GeK$), 0.64 (s, 6H, $Si(C\underline{H}_3)_2Si(CH_3)_3$), 3.25 (s, 24H, CH_2O). ^{13}C{^{1}H} NMR (75.43 MHz, 295.0 K, C_6D_6, δ ppm): 0.0 $(Si(CH_3)_2Si(\underline{C}H_3)_3)$, 3.5 $(Si(\underline{C}H_3)_2Si(CH_3)_3)$, 8.5 $(((\underline{C}H_3)_3Si)_2GeK)$, 70.0 (CH_2O). ^{29}Si{^{1}H} INEPT NMR (59.59 MHz, 295.0 K, C_6D_6, δ ppm): -33.0 $(\underline{Si}(CH_3)_2Si(CH_3)_3)$, -16.6 $(Si(CH_3)_2\underline{Si}(CH_3)_3)$, -3.4 $(((CH_3)_3\underline{Si})_2GeK)$. Mass required for $C_{13}H_{38}GeSi_4$ after ethylbromide derivatization: 380.1. Mass found after ethylbromide derivatization GC/MS: m/z (%) = 380 (1) [M^+]; 365 (1) [M^+-Me]; 350 (3) [M^+-Et-H]; 307 (1) [M^+-$SiMe_3$]; 292 (1) [M^+-$SiMe_3$-Me]; 277 (3) [M^+-$SiMe_3$-2Me]; 262 (1) [M^+-$SiMe_3$-3Me]; 234 (3) [M^+-2$SiMe_3$]; 219 (8) [M^+-2$SiMe_3$-Me]; 203 (17) [M^+-2$SiMe_3$-2Me-H]; 187 (6) [M^+-2$SiMe_3$-3Me-2H]; 159 (4) [M^+-3$SiMe_3$-H]; 145 (10) [M^+-3$SiMe_3$-Me]; 131 (33) [$GeSiC_2H_5^+$]; 115 (9) [$GeSiCH^+$]; 73 (100) [$SiMe_3^+$].

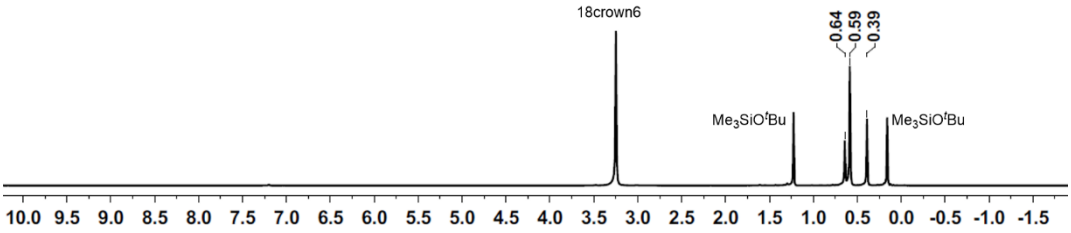

Figure S6a. ^{1}H NMR spectrum of the reaction mixture of the synthesis of germylpotassium compound 18-crown-6 (**20**) in C_6D_6.

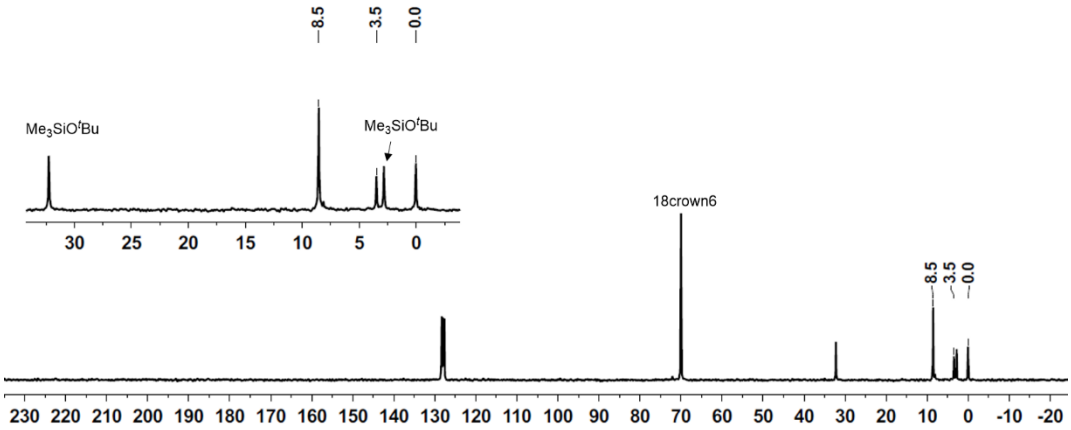

Figure S6b. ^{13}C{^{1}H} NMR spectrum of the reaction mixture of the synthesis of germylpotassium compound 18-crown-6 (**20**) in C_6D_6.

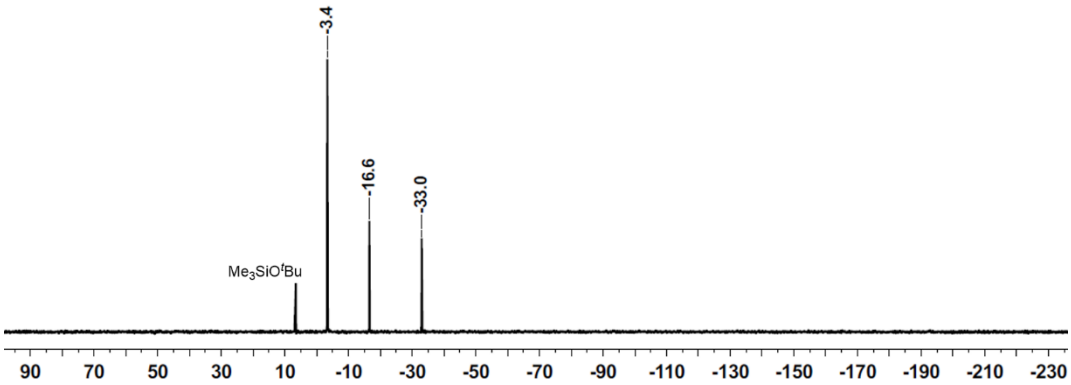

Figure S6c. ^{29}Si NMR spectrum of the reaction mixture of the synthesis of germylpotassium compound 18-crown-6 (**20**) in C_6D_6.

Bis(trimethylsilyl)pentamethyldisilanylgermane (16)

^{1}H NMR (499.87 MHz, 305.1 K, C_6D_6, δ ppm):): 0.22 (s, 9H, $Si(CH_3)_2Si(C\underline{H}_3)_3$), 0.35 (s, 18H, $((CH_3)_3Si)_2Ge$), 0.40 (s, 6H, $Si(C\underline{H}_3)_2Si(CH_3)_3$), 2.25 (s, 1H, $Ge\underline{H}$). ^{13}C{^{1}H} NMR (125.71 MHz, 305.0 K, $CDCl_3$, δ ppm): -1.7 ($Si(CH_3)_2Si(\underline{C}H_3)_2$), -1.6 ($Si(\underline{C}H_3)_3Si(CH_3)_2$), 3.1 ($((CH_3)_3Si)_2Ge$). ^{29}Si{^{1}H} NMR (99.31 MHz, 305.0 K, C_6D_6, δ ppm): -34.3 ($\underline{Si}(CH_3)_2Si(CH_3)_3$), -16.2 ($Si(CH_3)_2\underline{Si}(CH_3)_3$), -5.7 ($((CH_3)_3Si)_2Ge$). Mass required for $C_{11}H_{34}GeSi_4$: 352.1. Mass found GC/MS: 335 (2) [M^+-Me-2H]; 278 (27) [M^+-$SiMe_3$-H]; 263 (2) [M^+-$SiMe_3$-Me-H]; 203 (13) [M^+-2$SiMe_3$-2H]; 189 (10) [M^+-2$SiMe_3$-Me-2H]; 173 (2) [M^+-2$SiMe_3$-2Me-2H]; 131 (24) [$SiMe_3SiMe_2^+$]; 115 (14) [$Si_2C_4H_{11}^+$]; 73 (100) [$SiMe_3^+$]. IR (ATR, neat) $\nu_{Ge\text{-}H}$ 1951 cm^{-1}. Anal. found/calcd. for $C_{11}H_{34}GeSi_4$ C 38.85/37.60, H 9.41/9.75.

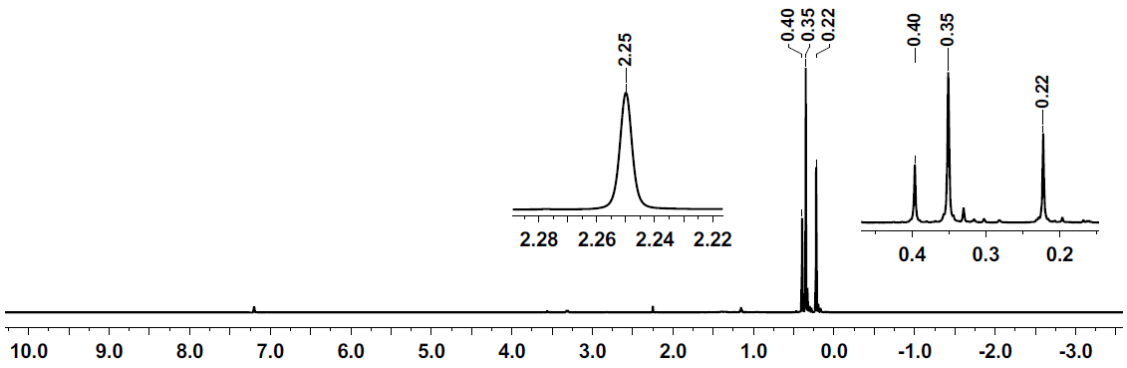

Figure S7a. ^{1}H NMR spectrum of bis(trimethylsilyl)pentamethyldisilanylgermane (**16**) in C_6D_6.

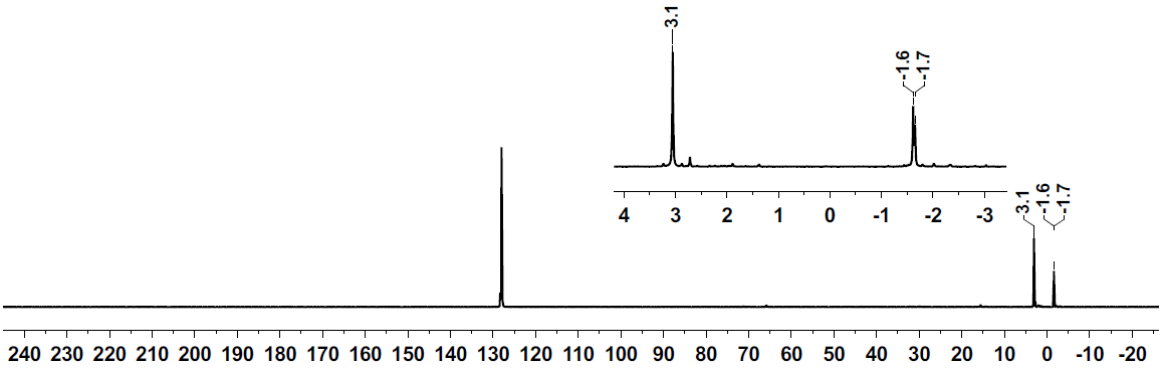

Figure S7b. $^{13}C\{^{1}H\}$ NMR spectrum of bis(trimethylsilyl)pentamethyldisilanylgermane (**16**) in C_6D_6.

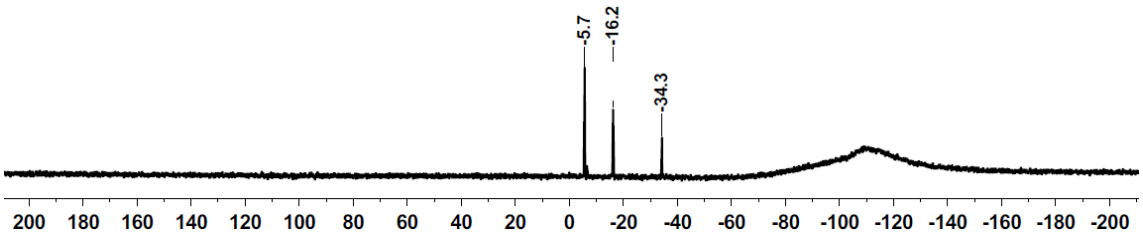

Figure S7c. $^{29}Si\{^{1}H\}$ NMR spectrum of bis(trimethylsilyl)pentamethyldisilanylgermane (**16**) in C_6D_6.

General preparation of trialkylsilyl arenium borates (10a-d)[11]

$$R_3SiH + [Ph_3C][B(C_6F_5)_4] \xrightarrow{\text{arene}} [R_3Si(\text{arene})][B(C_6F_5)_4]$$

Triphenylmethyl tetrakis(pentafluorophenyl)borate was dissolved in 3 mL of the indicated solvent and the silane was added. The formation of two phases could be observed and the biphasic reaction mixture was vigorously stirred for 30 min. The upper, non-polar phase was removed and the lower, polar phase was washed with 2 mL of the used solvent and again the non-polar phase was removed. The polar phase was dried under reduced pressure for 30 min and then dissolved in the respective deuterated solvent.

Triethylsilyl benzenium borate (10a) 0.50 g (0.54 mmol) Triphenylmethyl tetrakis(pentafluorophenyl)borate was dissolved in 3 mL benzene and 0.14 mL (1.6 eq., 0.87 mmol) triethylsilane was added.

Tri-*iso*-propylsilyl toluenium borate (10b) 0.46 g (0.50 mmol) Triphenylmethyl tetrakis(pentafluorophenyl)borate was dissolved in 3 mL toluene and 0.11 mL (1.1 eq., 0.55 mmol) tri-*iso*-propylsilane was added.

Trimethylsilyl toluenium borate (10c) 0.46 g (0.50 mmol) Triphenylmethyl tetrakis(pentafluorophenyl)borate was dissolved in 3 mL toluene and 0.06 mL (1.1 eq., 0.55 mmol) trimethylsilane was added.

General procedure for the rearrangement of tris(trimethylsilyl)silyltrimethylgermane (1) with trialkylsilyl arenium borates (10a-c)

A solution of 0.18 g (0.50 mmol) silagermane **1** in 1 mL of the named deuterated solvent was added to a precooled solution of the named trialkylsilyl arenium borate **10a-c**. The reaction mixture was stirred for 2 h at the specified temperature and then allowed to warm to room temperature. The polar phase and the non-polar phase were each transferred to separate NMR tubes to be analyzed independently. In the following reactions the NMR spectra of the polar phase showed too may signals to be analyzable but the compounds in the non-polar phase were identified by NMR and GC/MS spectroscopy.

Tris(trimethylsilyl)silyltrimethylgermane (1) with triethylsilyl benzenium borate (10a)

The reaction was performed at 6 °C in benzene-d_6.

Non-polar phase:

^{1}H NMR (499.87 MHz, 305.0 K, C_6D_6, δ ppm): 0.32-0.38 (m, 1H, CH_3), 0.78-0.92 (m, 0.19H, $C\underline{H}_2CH_3$), 1.04-1.11 (m, 0.27H, $CH_2C\underline{H}_3$). ^{13}C{^{1}H} NMR (125.69 MHz, 298.0 K, C_6D_6, δ ppm): 0.57 (CH_3), 0.64 (CH_3), 0.72 (CH_3), 0.80 (CH_3), 0.89 (CH_3), 3.47 (CH_3), 3.60 (CH_3), 3.73 (CH_3), 3.76 (CH_3), 3.86 (CH_3), 3.89 (CH_3), 4.02 (CH_3), 7.97 ($CH_2\underline{C}H_3$), 8.66 ($CH_2\underline{C}H_3$), 8.68 ($CH_2\underline{C}H_3$), 8.71 ($CH_2\underline{C}H_3$), 9.72 ($\underline{C}H_2CH_3$), 9.82 ($\underline{C}H_2CH_3$), 11.45 ($\underline{C}H_2CH_3$), 11.52 ($\underline{C}H_2CH_3$), 11.58 ($\underline{C}H_2CH_3$), 11.65 ($\underline{C}H_2CH_3$), 11.72 ($\underline{C}H_2CH_3$). ^{29}Si{^{1}H} INEPT NMR (99.31 MHz, 305.0 K, C_6D_6, δ ppm): -5.13, -5.10, -1.39, -1.37, -1.30, -1.27, -1.23.

GC/MS:

rt = 3.58 min, tetramethylsilane

m/z (%) = 88.0 (2) [M^+], 73.0 (100) [M^+-Me].

rt = 4.1 min, ethyltrimethylsilane

m/z (%) = 101.0 (4) [M^+], 87.0 (47) [M^+-Me], 73.0 (97) [M^+-2Me], 58.0 (100) [M^+-3Me].

rt = 5.18 min, diethyldimethylsilane

m/z (%) = 116 (4) [M^+], 101.0 (11) [M^+-Me], 87.0 (92) [M^+-2Me], 73.0 (13) [M^+-3Me], 58.0 (100) [M^+-4Me].

rt = 18.1 min, **(2)**

m/z (%): 366.1 (32) [M^+], 351.1 (18) [M^+-Me], 278.0 (27) [M^+-$SiMe_3$-Me], 219.0 (30) [$C_6H_{17}GeSi_2^+$], 203.0 (16) [$C_5H_{13}GeSi_2^+$], 145.0 (28) [$C_3H_7GeSi^+$], 131.0 (49) [$C_2H_6GeSi^+$], 73.0 (100) [$SiMe_3^+$].

rt = 19.5 min, **(11**, n = 3**)**

m/z (%): 380.0 (48) [M^+], 365.0 (10) [M^+-Me], 292.0 (72) [M^+-$SiMe_3$-Me], 278.0 (93) [$C_8H_{24}GeSi_3^+$], 264.0 (24) [$C_7H_{22}GeSi_3^+$], 145.0 (25) [$C_3H_7GeSi^+$], 131.0 (44) [$C_2H_6GeSi^+$], 87.0 (43) [$C_4H_{11}Si^+$], 73.0 (100) [$SiMe_3^+$].

rt = 20.8 min, **(11**, n = 2**)**

m/z (%): 394.0 (44) [M^+], 379.0 (10) [M^+-Me], 306.0 (31) [M^+-$SiMe_3$-Me], 292.0 (100) [$C_9H_{26}GeSi_3^+$], 278.0 (45) [$C_8H_{24}GeSi_3^+$], 264.0 (26) [$C_7H_{22}GeSi_3^+$], 131.0 (32) [$C_2H_6GeSi^+$], 87 (70) [$C_4H_{11}Si^+$], 73 (80) [$SiMe_3^+$], 57 (73) [$C_2H_5Si^+$].

rt = 21.9 min, **(11**, n = 1**)**

m/z (%): 408.2 (43) [M^+], 306.0 (90) [$C_{10}H_{28}GeSi_3^+$], 292.0 (80) [$C_9H_{26}GeSi_3^+$], 278.0 (40) [$C_8H_{24}GeSi_3^+$], 131.0 (28) [$C_2H_6GeSi^+$], 87.0 (100) [$C_4H_{11}Si^+$], 73.0 (68) [$SiMe_3^+$], 57.0 (94) [$C_2H_5Si^+$].

rt = 23.0 min, **(11**, n = 0**))**

m/z (%): 422.2 (39) [M^+], 320.0 (51) [$C_{11}H_{30}GeSi_3^+$], 306.0 (93) [$C_{10}H_{28}GeSi_3^+$], 292.0 (49) [$C_9H_{26}GeSi_3^+$], 278.0 (33) [$C_8H_{24}GeSi_3^+$], 131.0 (25) [$C_2H_6GeSi^+$], 101.0 (39) [$C_5H_{13}Si^+$], 87.0 (100) [$C_4H_{11}Si^+$], 73.0 (59) [$SiMe_3^+$], 57.0 (97) [$C_2H_5Si^+$].

rt = 24.0 min, **(12)**

m/z (%): 436.2 (39) [M^+], 407.0 (10) [$C_{15}H_{41}GeSi_4$+], 334.0 (32) [$C_{12}H_{32}GeSi_3^+$], 320.0 (100) [$C_{11}H_{30}GeSi_3^+$], 306.0 (60) [$C_{10}H_{28}GeSi_3^+$], 292.0 (47) [$C_9H_{26}GeSi_3^+$], 278.0 (20) [$C_8H_{24}GeSi_3^+$], 131.0 (21) [$C_2H_6GeSi^+$], 101.0 (74) [$C_5H_{13}Si^+$], 87 (96) [$C_4H_{11}Si^+$], 73 (78) [$SiMe_3^+$], 57 (100) [$C_2H_5Si^+$].

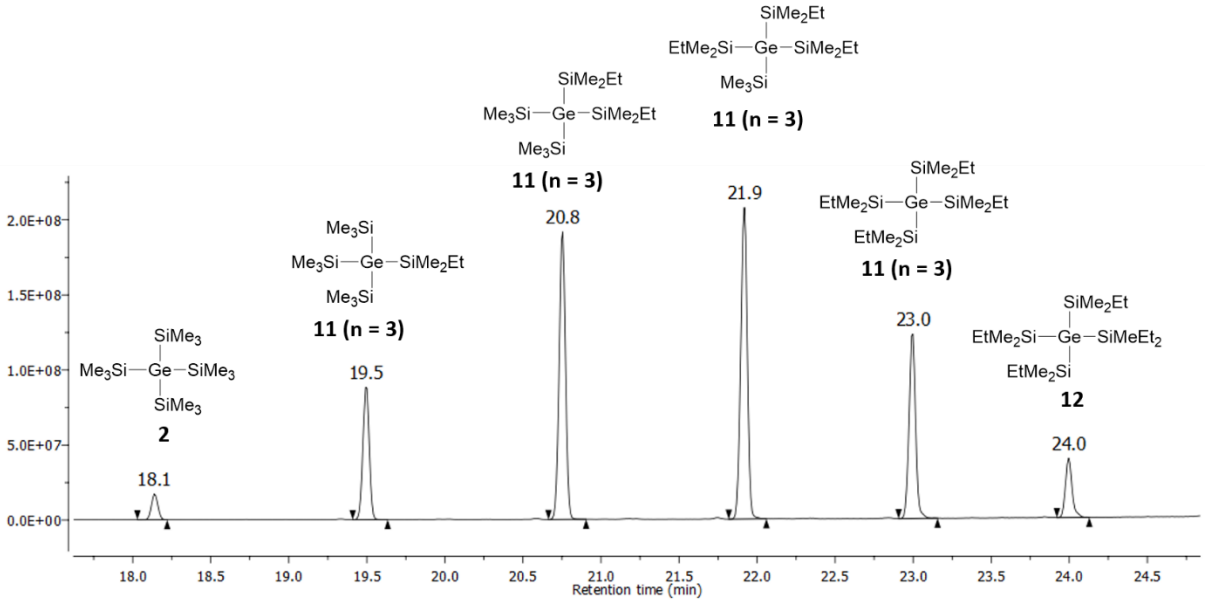

Figure S8. Part of the GC trace of the non-polar phase of the reaction of tris(trimethylsilyl)silyltrimethyl-germane (**1**) with triethylsilyl benzenium borate (**10a**).

Tris(trimethylsilyl)silyltrimethylgermane (1) with tri-*iso*-propylsilyl toluenium borate (10b)

The reaction was performed at -15 °C in toluene-d_8.

Non-polar phase

$^{29}Si\{^1H\}$ NMR (99.31 MHz, 305.0 K, C_6D_6, δ ppm)[12]: -5.1 ($((CH_3)_3Si)_4Ge$), -4.5 ($((CH_3)_2((CH_3)_2CH)SiGe(\underline{Si}(CH_3)_3)_3$), 5.1 ($((CH_3)_2((CH_3)_2CH)\underline{Si}Ge(Si(CH_3)_3)_3$), 9.0 ($(((CH_3)_2CH)_3SiCH_3$).

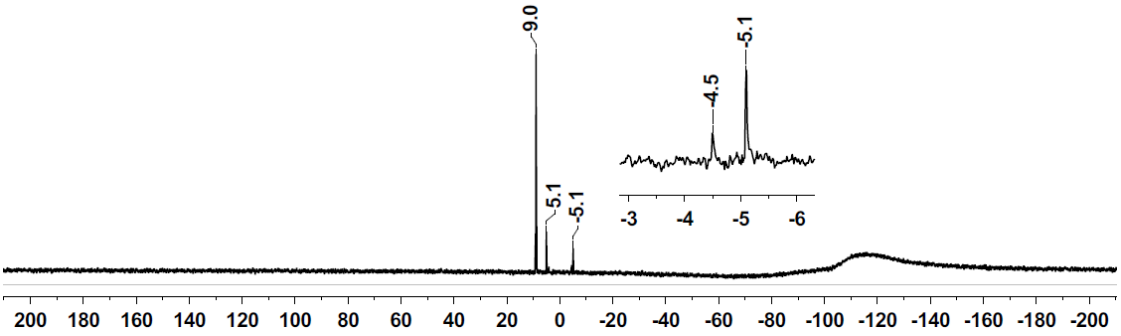

Figure S9. $^{29}Si\{^{1}H\}$ NMR spectrum of the non-polar phase of the reaction of tris(trimethylsilyl)silyltrimethyl-germane (**1**) with tri-*iso*-propylsilyl toluenium borate (**10b**).

GC-MS:

rt = 8.2 min, $^{i}Pr_3SiMe$

m/z (%): 172.2 (5) [M^+], 157.2 (1) [M^+-Me], 129.1 (100) [M^+-^{i}Pr], 115.1 (1) [M^+-^{i}Pr-Me], 101.0 (17) [M^+-^{i}Pr-2Me], 87.0 (45) [M^+-2^{i}Pr].

rt = 15.4 min, **(2)**

m/z (%): 366.2 (12) [M^+], 351.1 (10) [M^+-Me], 278.0 (55) [M^+-$SiMe_3$-Me], 219.0 (17) [$C_6H_{17}GeSi_2^+$], 204.0 (15) [$C_5H_{14}GeSi_2^+$], 145.0 (20) [$C_3H_7GeSi_+$], 131.0 (40) [$C_2H_6GeSi^+$], 73.0 (100) [$SiMe_3^+$].

rt = 17.9 min, $(Me_3Si)_3GeSiMe_2{}^{i}Pr$

m/z (%): 394.0 (14) [M^+], 351.1 (14) [$C_{11}H_{33}GeSi_4$], 278.0 (48) [$C_8H_{24}GeSi_3^+$], 203.0 (28) [$C_5H_{13}GeSi_2^+$], 131.0 (27) [$C_2H_6GeSi^+$], 73.0 (100) [$SiMe_3^+$].

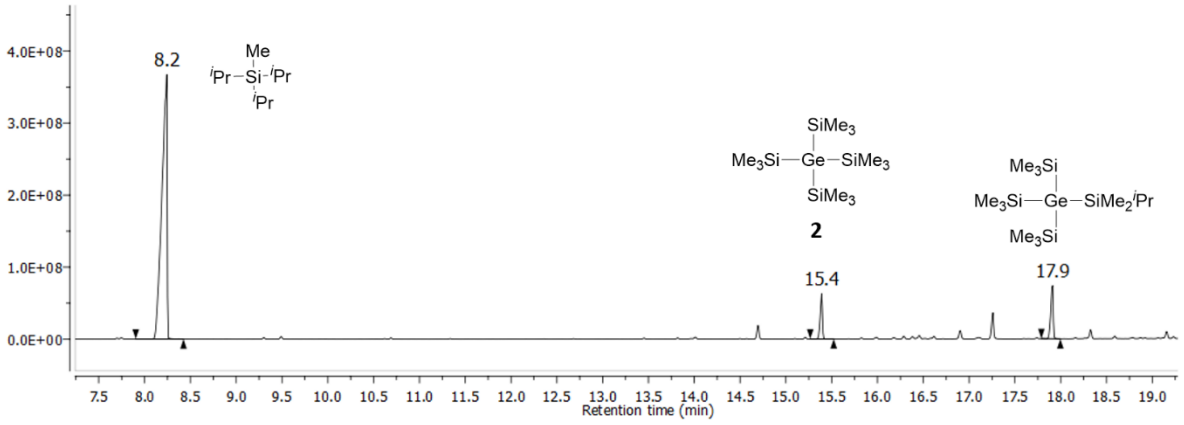

Figure S10. Part of the GC trace of the non-polar phase of the reaction tris(trimethylsilyl)silyltrimethylgermane (**1**) with tri-*iso*-propylsilyl toluenium borate (**10b**).

Tris(trimethylsilyl)silyltrimethylgermane (1) with trimethylsilyl toluenium borate (10c)

The reaction was performed at 0 °C in toluene-d_8.

Non-polar phase

^{1}H NMR (499.87 MHz, 297.0 K, C_6D_6, δ ppm): 0.0 ($(CH_3)_4Si$), 0.26 ($(CH_3)_3Si)_4Ge$). $^{13}C\{^{1}H\}$ NMR (125.70 MHz, 299.0 K, C_7D_8, δ ppm): 0.0 ($(CH_3)_4Si$), 3.6 ($((CH_3)_3Si)_4Ge$). $^{29}Si\{^{1}H\}$ NMR (99.31 MHz, 295.5 K, C_7D_8, δ ppm): -5.1 ($((CH_3)_3Si)_4Ge$), 0.0 ($(CH_3)_4Si$).

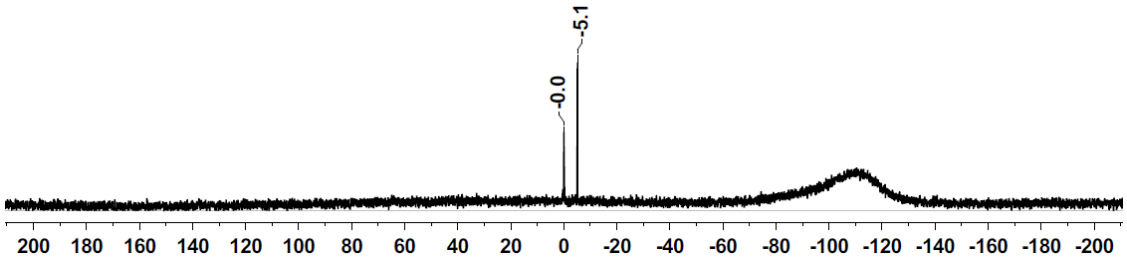

Figure S11. $^{29}Si\{^{1}H\}$ NMR spectrum of the non-polar phase of the reaction of tris(trimethylsilyl)silyltrimethyl-germane (**1**) with trimethylsilyl toluenium borate (**10c**).

Rearrangement of tris(trimethylsilyl)silyldimethylgermyl toluenium borate ($3(C_7D_8)[B(C_6F_5)_4]$) to tris(trimethyl-silyl)germyldimethylsilyl toluenium borate ($8(C_7D_8)[B(C_6F_5)_4]$) starting from silagermane (1)

To a solution of 0.18 g (0.50 mmol) tris(trimethylsilyl)silyltrimethylgermane **1** in 1 mL toluene-d_8 cooled to -20°C 1 eq. tri-*iso*-propylsilyl toluenium borate **10b** was slowly added via a Teflon tube. The mixture was stirred for 1 h at -20 °C. The brown polar phase and the light yellow non-polar phase were each transferred to separate NMR tubes at -20 °C and stored at -60 °C overnight until the NMR spectra were recorded the next morning. The polar phase contained borates [**3**(C_7D_8)][$B(C_6F_5)_4$] and [**8**(C_7D_8)][$B(C_6F_5)_4$]). The non-polar phase contained methyl-tri-*iso*-propylsilane and the rearrangement product **2**.

Polar phase:

^{1}H NMR (499.87 MHz, 253.0 K, C_7D_8, δ ppm): -0.15 ($((CH_3)_3Si)_3GeSi(C\underline{H}_3)_2^+$), 0.07 ($((C\underline{H}_3)_3Si)_3GeSi(CH_3)_2^+$), 0.12 ($((C\underline{H}_3)_3Si)_3SiGe(CH_3)_2^+$), 0.28 ($((CH_3)_3Si)_3SiGe(C\underline{H}_3)_2^+$). $^{13}C\{^{1}H\}$ NMR (125.71 MHz, 253.0 K, C_7D_8, δ ppm): 1.6 ($((\underline{C}H_3)_3Si)_3SiGe(CH_3)_2^+$), 2.5 ($((\underline{C}H_3)_3Si)_3GeSi(CH_3)_2^+$), 5.5 ($((CH_3)_3Si)_3GeSi(\underline{C}H_3)_2^+$), 12.1 ($((CH_3)_3Si)_3SiGe(\underline{C}H_3)_2^+$). $^{29}Si\{^{1}H\}$ NMR (99.31 MHz, 253.0 K, C_7D_8, δ ppm): -87.9 ($((CH_3)_3Si)_3\underline{Si}Ge(CH_3)_2^+$), -7.9 ($((CH_3)_3\underline{Si})_3SiGe(CH_3)_2^+$), -2.4 ($((CH_3)_3\underline{Si})_3GeSi(CH_3)_2^+$), 98.1 ($((CH_3)_3Si)_3Ge\underline{Si}(CH_3)_2^+$).

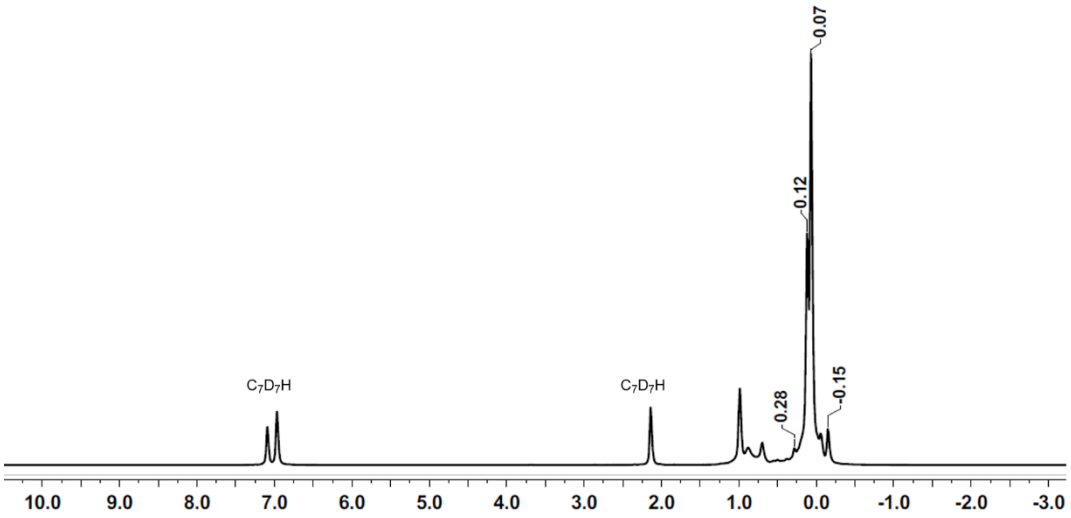

Figure S12a. ^{1}H NMR spectrum obtained from the polar phase of the reaction of silagermane **1** with tri-*iso*-propyl-silyl toluenium borate (**10b**) after 1h at -20°C.

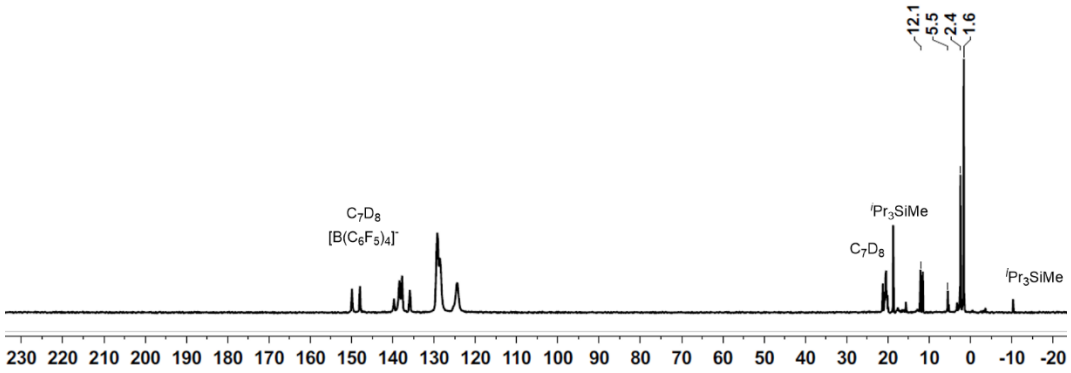

Figure S12b. ^{13}C{^{1}H} NMR spectrum obtained from the polar phase of the reaction of silagermane **1** with tri-*iso*-propylsilyl toluenium borate (**10b**) after 1h at -20°C.

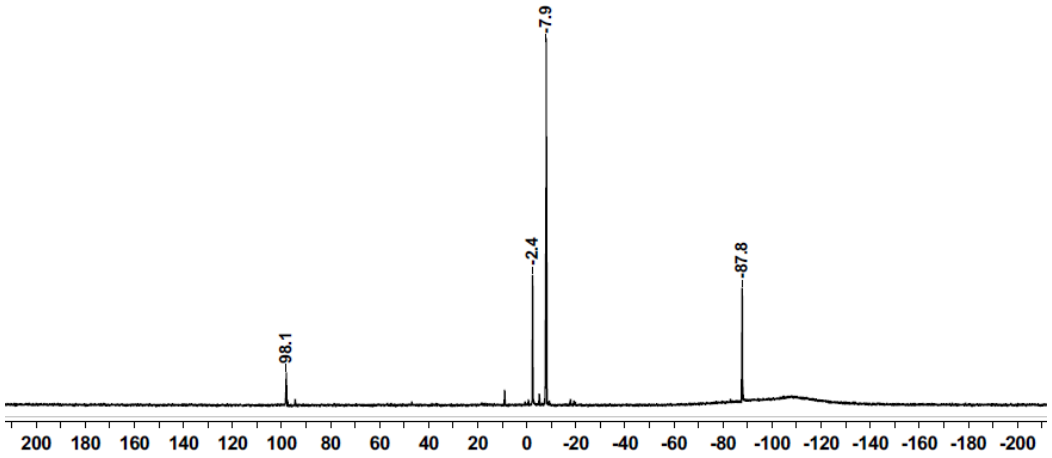

Figure S12c. ^{29}Si{^{1}H} NMR spectrum obtained from the polar phase of the reaction of silagermane **1** with tri-*iso*-propylsilyl toluenium borate (**10b**) after 1h at -20°C.

Non-polar phase:

^{1}H NMR (499.87 MHz, 305.0 K, C_7D_8, δ ppm): -0.17 (s, $((CH_3)_2CH)_3SiC\underline{H}_3$), 0.26 (s, $((CH_3)_3Si)_4Ge$), 0.86 (sept, $^{3}J_{H,H}$ = 7.3 Hz, $((CH_3)_2C\underline{H})_3SiCH_3$), 0.97 (d, $^{3}J_{H,H}$ = 7.3 Hz, $((C\underline{H}_3)_2CH)_3SiCH_3$). $^{13}C\{^{1}H\}$ NMR (127.71 MHz, 305.0 K, C_7D_8, δ ppm): -10.1 $(((CH_3)_2CH)_3Si\underline{C}H_3)$, 3.5 $(((CH_3)_3Si)_4Ge)$, 11.8 $(((CH_3)_2CH)_3SiCH_3)$, 18.8 $(((CH_3)_2CH)_3SiCH_3)$. $^{29}Si\{^{1}H\}$ NMR (99.31 MHz, 305.0 K, C_7D_8, δ ppm): -5.1 $(((CH_3)_3Si)_4Ge)$, 9.0 $(((CH_3)_2CH)_3SiCH_3)$.

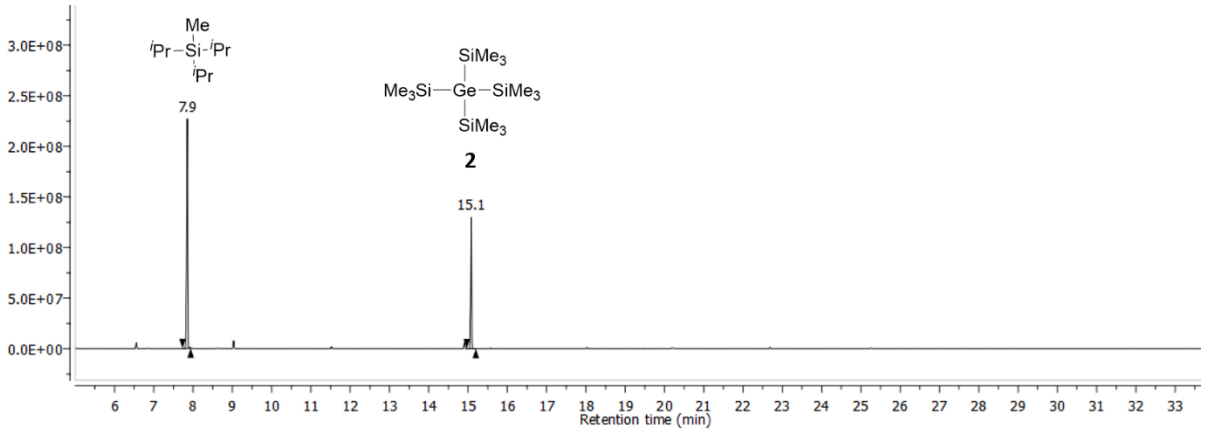

Figure S13a. Part of the GC trace obtained from the non-polar phase of the reaction of silagermane **1** with tri-*iso*-propylsilyl toluenium borate (**10b**) after 1h at -20°C.

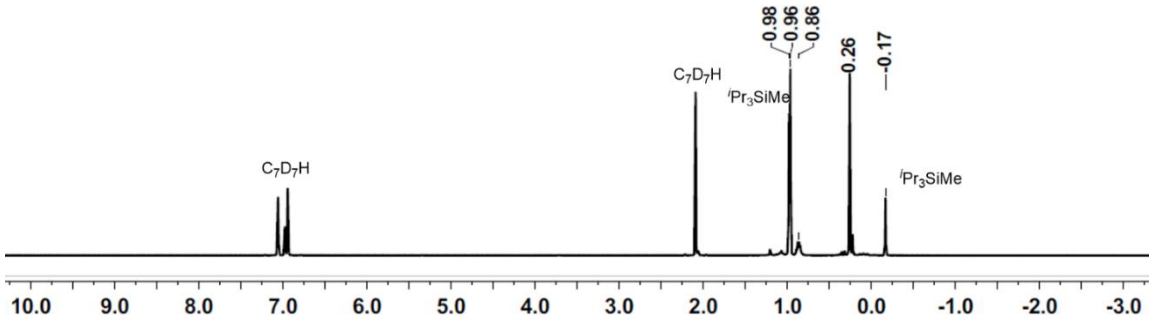

Figure S13b. ^{1}H NMR spectrum obtained from the non-polar phase of the reaction of silagermane **1** with tri-*iso*-propylsilyl toluenium borate (**10b**) after 1h at -20°C.

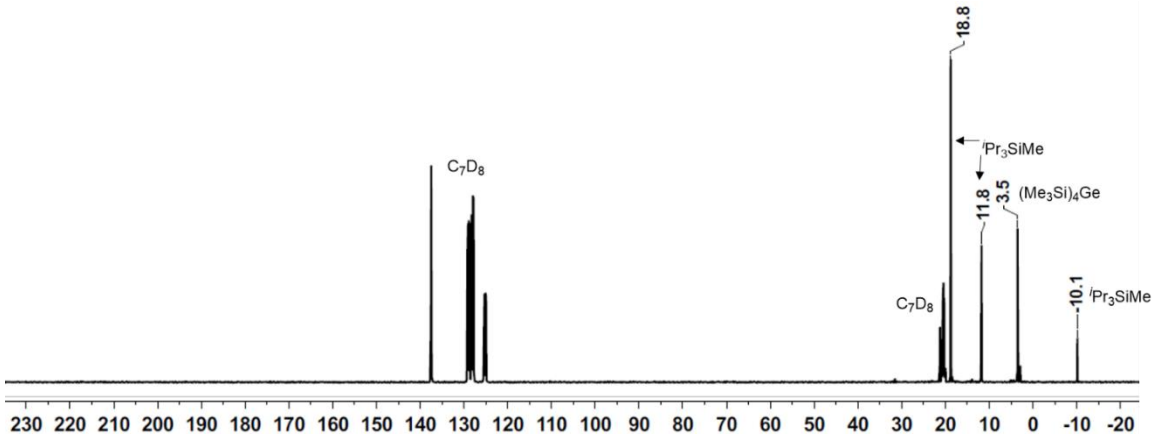

Figure S13c. $^{13}C\{^{1}H\}$ NMR spectrum obtained from the non-polar phase of the reaction of silagermane **1** with tri-*iso*-propylsilyl toluenium borate (**10b**) after 1h at -20°C.

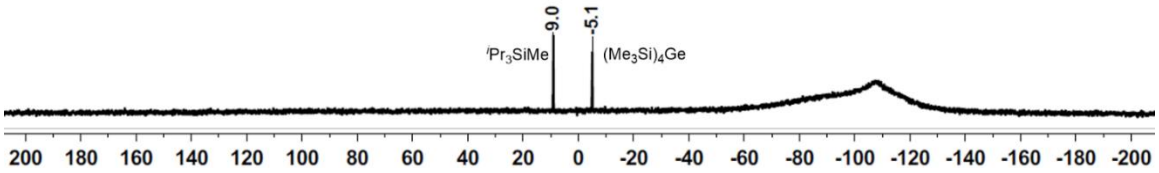

Figure S13d. $^{29}Si\{^{1}H\}$ NMR spectrum obtained from the non-polar phase of the reaction of silagermane **1** with tri-*iso*-propylsilyl toluenium borate (**10b**) after 1h at -20°C.

Rearrangement of tris(trimethylsilyl)silyldimethylgermyl toluenium borate ($3(C_7D_8)[B(C_6F_5)_4]$) to tris(trimethylsilyl)germyldimethylsilyl toluenium borate ($8(C_7D_8)[B(C_6F_5)_4]$) starting from hydrogen substituted silagermane (14)

0.14 g (0.40 mmol) tris(trimethylsilyl)silyldimethylgermane **14** and 0.37 g (0.40 mmol) triphenylmethyl tetrakis(pentafluorophenyl)borate were each dissolved in 1 mL toluene-d_8 and cooled to -20 °C. Silagermane **14** was slowly added to the borate salt via a Teflon tube and the mixture was stirred at -20 °C for 1.5 h. The brown polar phase and the light yellow non-polar phase were each transferred to NMR tubes at -20 °C. The NMR spectra were recorded at -20 °C. The polar phase contained borates [**3**(C_7D_8)][$B(C_6F_5)_4$] and [**8**(C_7D_8)][$B(C_6F_5)_4$]). The non-polar phase contained triphenylmethane and the rearrangement product **2**.

Polar phase:

^{1}H NMR (499.87 MHz, 253.0 K, C_7D_8, δ ppm): -0.15 ($(\underline{C}H_3)_3Si)_3GeSi(C\underline{H}_3)_2^+$), 0.07 ($((C\underline{H}_3)_3Si)_3SiGe(CH_3)_2^+$), 0.12 ($((C\underline{H}_3)_3Si)_3GeSi(CH_3)_2^+$), 0.28 ($((CH_3)_3Si)_3SiGe(C\underline{H}_3)_2^+$). $^{13}C\{^{1}H\}$ NMR (125.71 MHz, 253.0 K, C_7D_8, δ ppm): 1.6 ($((\underline{C}H_3)_3Si)_3SiGe(CH_3)_2^+$), 2.4 ($((\underline{C}H_3)_3Si)_3GeSi(CH_3)_2^+$), 5.5 ($((CH_3)_3Si)_3GeSi(\underline{C}H_3)_2^+$), 12.1 ($((CH_3)_3Si)_3SiGe(\underline{C}H_3)_2^+$). $^{29}Si\{^{1}H\}$ NMR (99.31 MHz, 253.0 K, C_7D_8, δ ppm): -87.9 ($((CH_3)_3Si)_3\underline{Si}Ge(CH_3)_2^+$), -7.9 ($((CH_3)_3\underline{Si})_3SiGe(CH_3)_2^+$), -2.4 ($(CH_3)_3\underline{Si})_3GeSi(CH_3)_2^+$)), 98.1 ($((CH_3)_3Si)_3Ge\underline{Si}(CH_3)_2^+$).

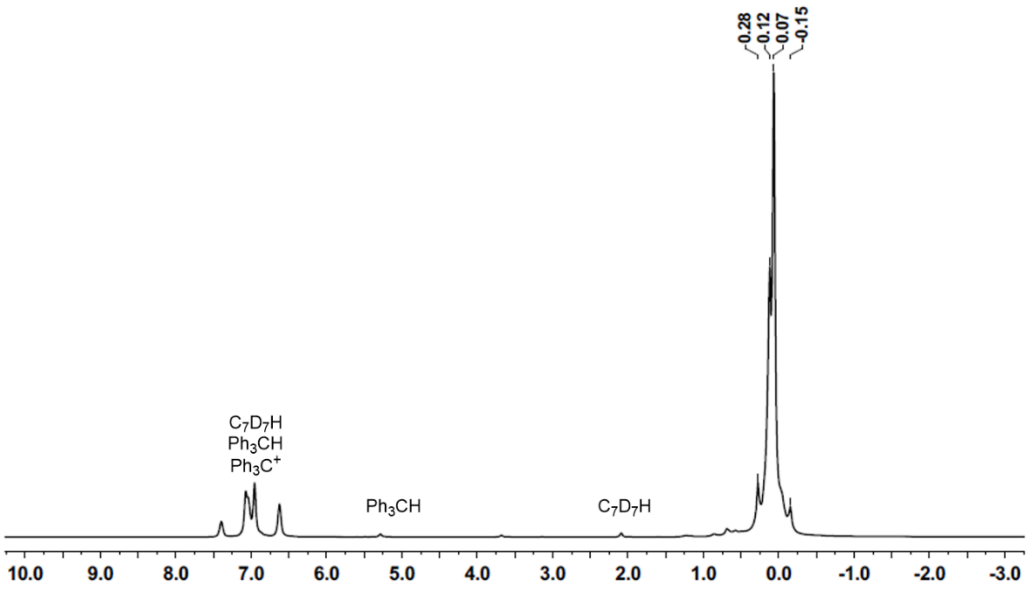

Figure S14a. ^{1}H NMR spectrum obtained from the polar phase of the reaction of germane **14** with $[Ph_3C][B(C_6F_5)_4]$ after 2h at -20°C.

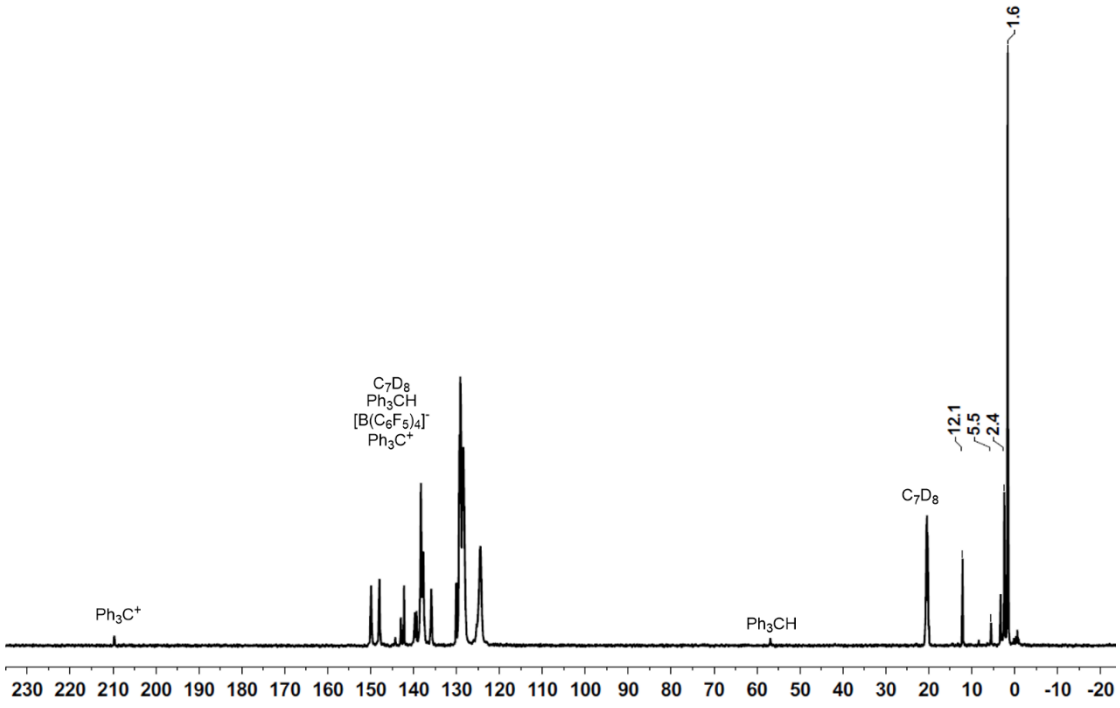

Figure S14b. $^{13}C\{^{1}H\}$ NMR spectrum obtained from the polar phase of the reaction of germane **14** with $[Ph_3C][B(C_6F_5)_4]$ after 2h at -20°C.

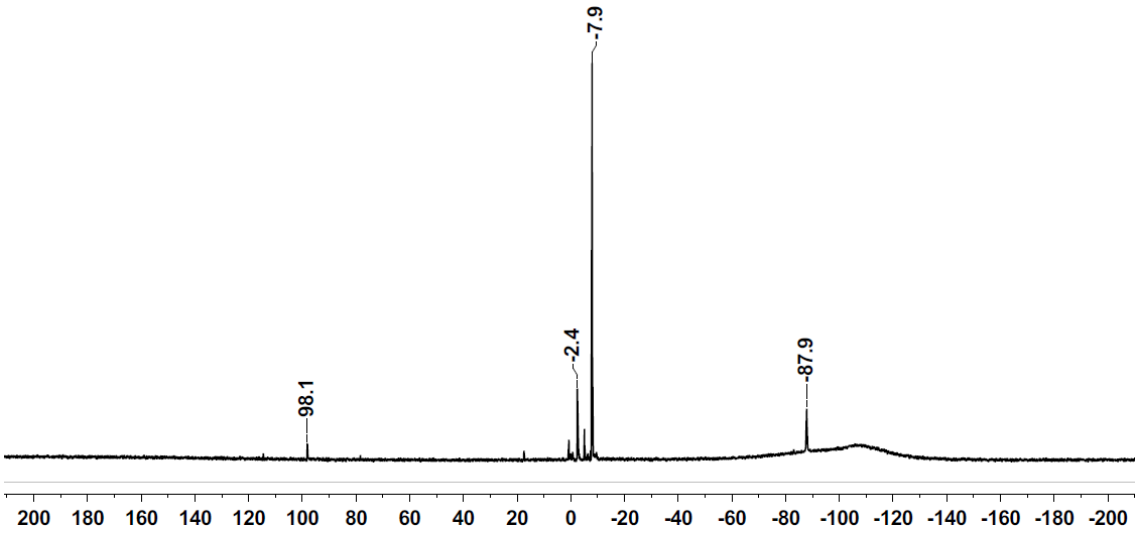

Figure S14c. $^{29}Si\{^{1}H\}$ NMR spectrum obtained from the polar phase of the reaction of germane **14** with $[Ph_3C][B(C_6F_5)_4]$ after 2h at -20°C.

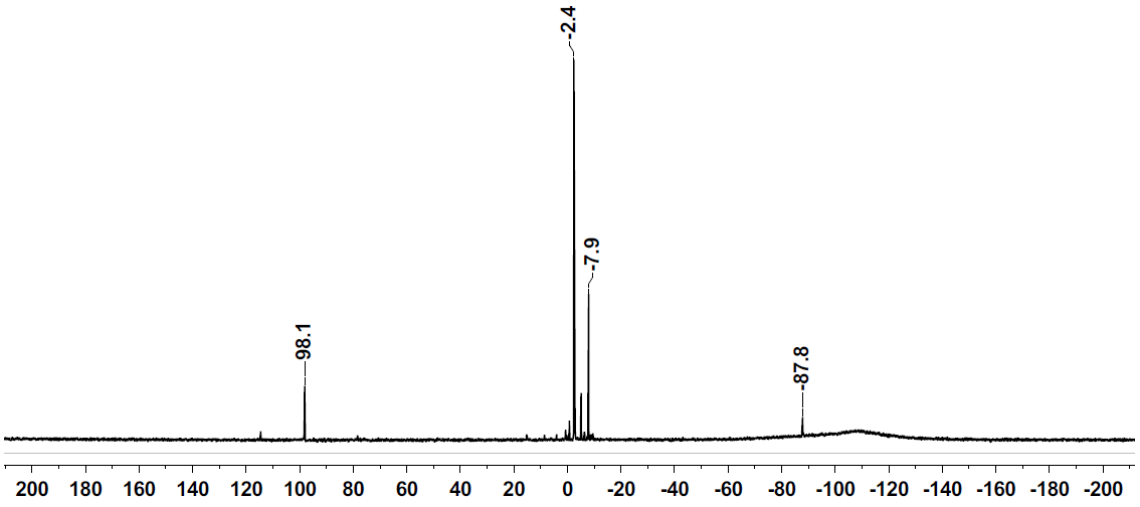

Figure S15a. $^{29}Si\{^{1}H\}$ NMR spectrum obtained from the polar phase of the reaction of germane **14** with $[Ph_3C][B(C_6F_5)_4]$ after 20h at -20°C.

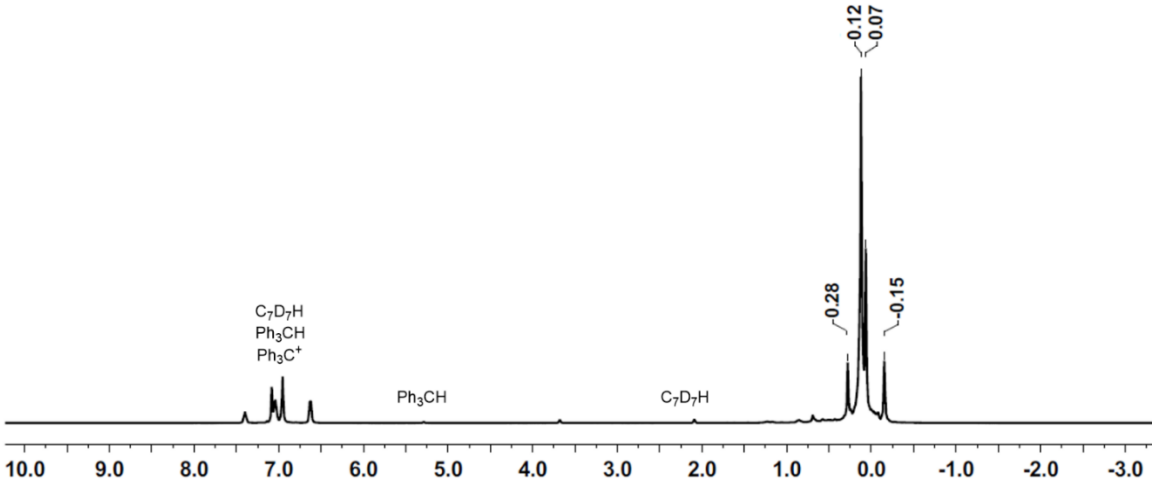

Figure S15b. ^{1}H NMR spectrum obtained from the polar phase of the reaction of germane **14** with $[Ph_3C][B(C_6F_5)_4]$ after 20h at -20°C.

Non-polar phase:

^{1}H NMR (499.87 MHz, 305.0 K, C_7D_8, δ ppm): 0.30 (s, $((CH_3)_3Si)_4Ge$), 5.38 (s, $Ph_3C\underline{H}$), 6.98-7.09 (m, $\underline{Ph}_3CH$). $^{13}C\{^{1}H\}$ NMR (127.71 MHz, 305.0 K, C_7D_8, δ ppm): 3.5 $((CH_3)_3Si)_4Ge$), 57.1 ($Ph_3\underline{C}H$), 125.4 ($\underline{Ph}_3CH$), 128.3 ($\underline{Ph}_3CH$), 129.2 ($\underline{Ph}_3CH$), 144.3 ($\underline{Ph}_3CH$). $^{29}Si\{^{1}H\}$ NMR (99.31 MHz, 305.0 K, C_7D_8, δ ppm): -5.1 $((CH_3)_3Si)_4Ge$).

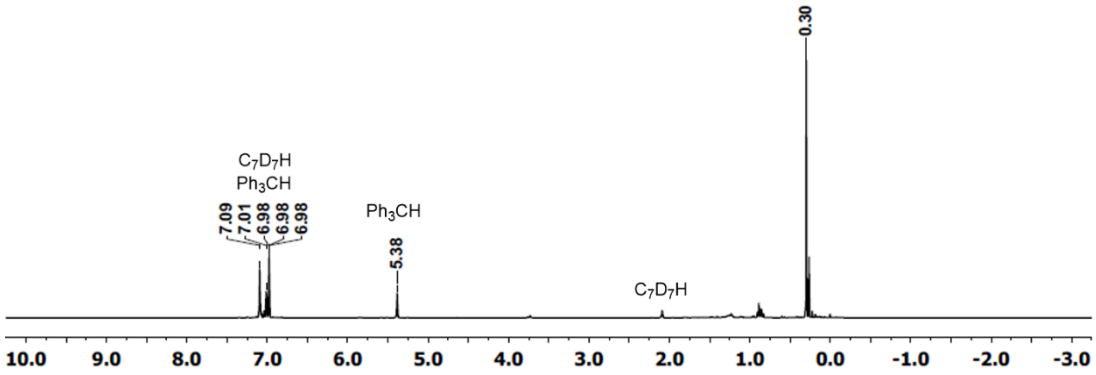

Figure S16a. ^{1}H NMR spectrum obtained from the non-polar phase of the reaction of germane **14** with $[Ph_3C][B(C_6F_5)_4]$ after 20h at -20°C.

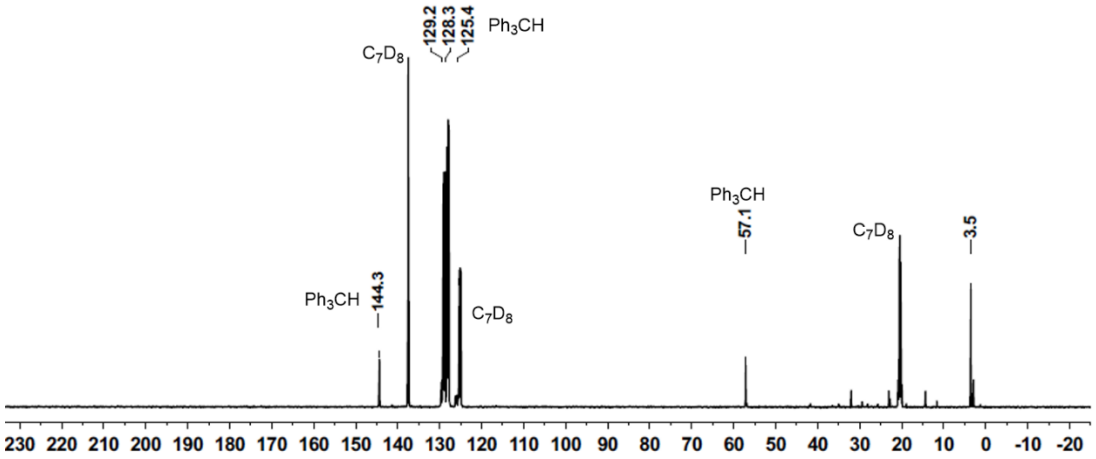

Figure S16b. $^{13}C\{^{1}H\}$ NMR spectrum obtained from the non-polar phase of the reaction of germane **14** with $[Ph_3C][B(C_6F_5)_4]$ after 20h at -20°C.

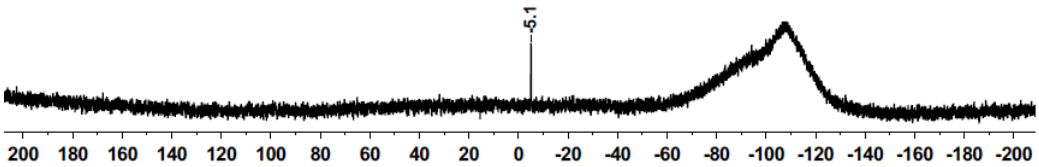

Figure S16c. $^{29}Si\{^{1}H\}$ NMR spectrum obtained from the non-polar phase of the reaction of germane **14** with $[Ph_3C][B(C_6F_5)_4]$ after 20h at -20°C. The signal is due to the product germane **2**.

Tris(trimethylsilyl)germyldimethylsilyl toluenium borate (8(C_7H_8)[$B(C_6F_5)_4$]) from silane 15

0.18 g (0.50 mmol) tris(trimethylsilyl)germyldimethylsilane **15** and 0.46 g (0.50 mmol) triphenylmethyl tetrakis(pentafluorophenyl)borate were both dissolved in 1 mL toluene-d_8 and cooled to -20 °C. Germylsilane **15** was slowly added to the borate salt via a Teflon tube and the mixture was stirred at -20 °C for 1.5 h. The brown polar phase and the light yellow non-polar phase were each transferred to separate NMR tubes at -20 °C and stored at -60 °C overnight until the NMR spectra were recorded the next morning. The polar phase contained borate [**8**(C_7D_8)][$B(C_6F_5)_4$]. The non-polar phase contained triphenylmethane and the rearrangement product **2**.

Polar phase:

^{1}H NMR (499.87 MHz, 253.0 K, C_7D_8, δ ppm): -0.15 (((CH$_3$)$_3$Si)$_3$GeSi(C<u>H</u>$_3$)$_2^+$), 0.12 (((C<u>H</u>$_3$)$_3$Si)$_3$GeSi(CH$_3$)$_2^+$). ^{13}C{^{1}H} NMR (125.71 MHz, 253.0 K, C_7D_8, δ ppm): 2.5 (((<u>C</u>H$_3$)$_3$Si)$_3$GeSi(CH$_3$)$_2^+$), 5.5 (((CH$_3$)$_3$Si)$_3$GeSi(<u>C</u>H$_3$)$_2^+$). ^{29}Si{^{1}H} NMR (99.31 MHz, 253.0 K, C_7D_8, δ ppm): -2.4 (((CH$_3$)$_3$<u>Si</u>)$_3$GeSi(CH$_3$)$_2^+$), 98.1 (((CH$_3$)$_3$Si)$_3$Ge<u>Si</u>(CH$_3$)$_2^+$).

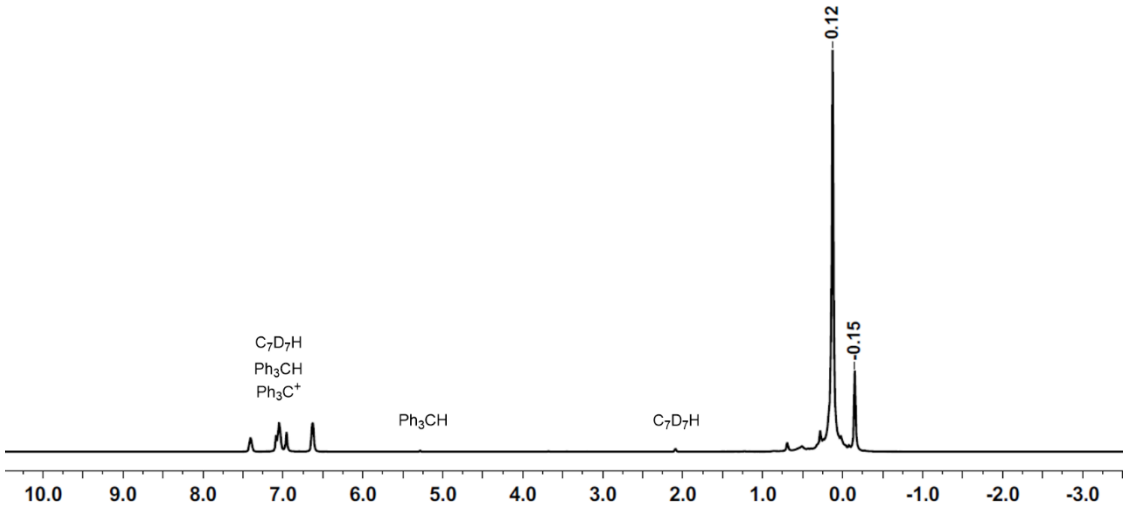

Figure S17a. ^{1}H NMR spectrum obtained from the polar phase of the reaction of silane **15** with [Ph_3C][$B(C_6F_5)_4$] after 1.5h at -20°C.

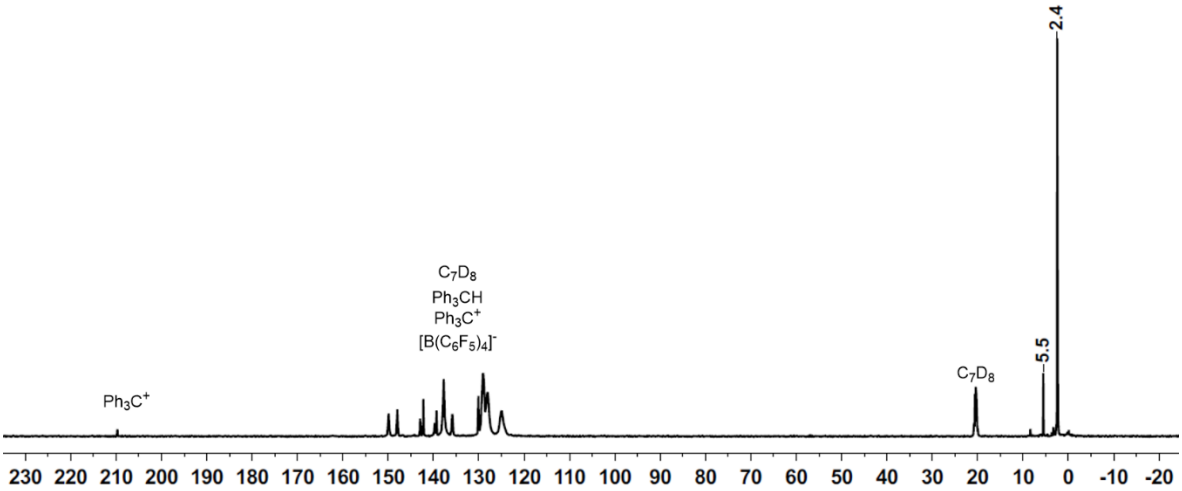

Figure S17b. ^{13}C{^{1}H} NMR spectrum obtained from the polar phase of the reaction of silane **15** with [Ph_3C][$B(C_6F_5)_4$] after 1.5h at -20°C.

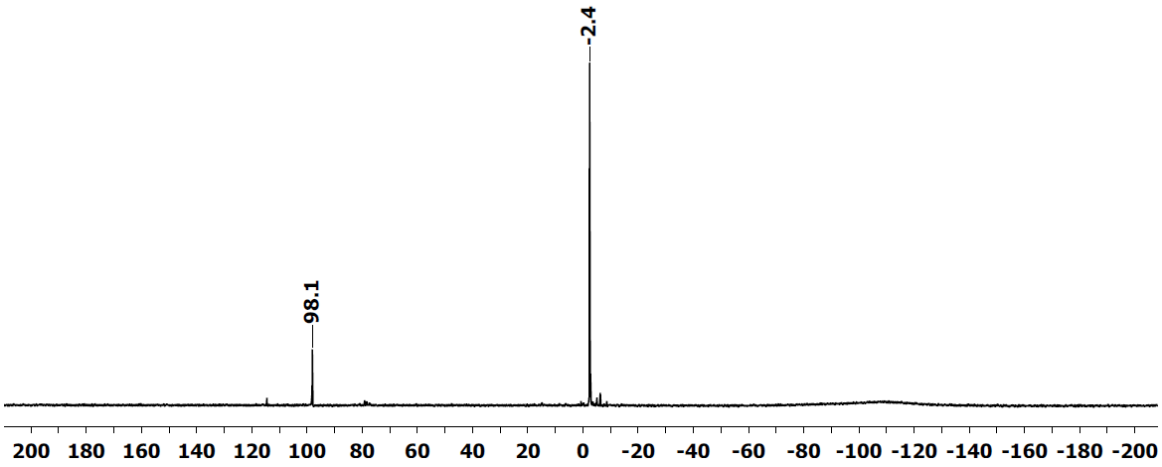

Figure S17c. $^{29}Si\{^{1}H\}$ NMR spectrum obtained from the polar phase of the reaction of silane **15** with $[Ph_3C][B(C_6F_5)_4]$ after 1.5h at -20°C.

Non-polar phase:

^{1}H NMR (499.87 MHz, 305.0 K, C_7D_8, δ ppm): 0.29 (s, $((CH_3)_3Si)_4Ge$), 5.38 (s, $Ph_3C\underline{H}$), 6.98-7.10 (m, $\underline{Ph}_3CH$). $^{13}C\{^{1}H\}$ NMR (125.69 MHz, 305.0 K, C_7D_8, δ ppm): 3.5 ($((CH_3)_3Si)_4Ge$), 57.2 ($Ph_3\underline{C}H$), 125.4 ($\underline{Ph}_3CH$), 128.3 ($\underline{Ph}_3CH$), 129.2 ($\underline{Ph}_3CH$), 144.3 ($\underline{Ph}_3CH$). $^{29}Si\{^{1}H\}$ NMR (99.31 MHz, 305.0 K, C_7D_8, δ ppm): -5.1 ($((CH_3)_3Si)_4Ge$).

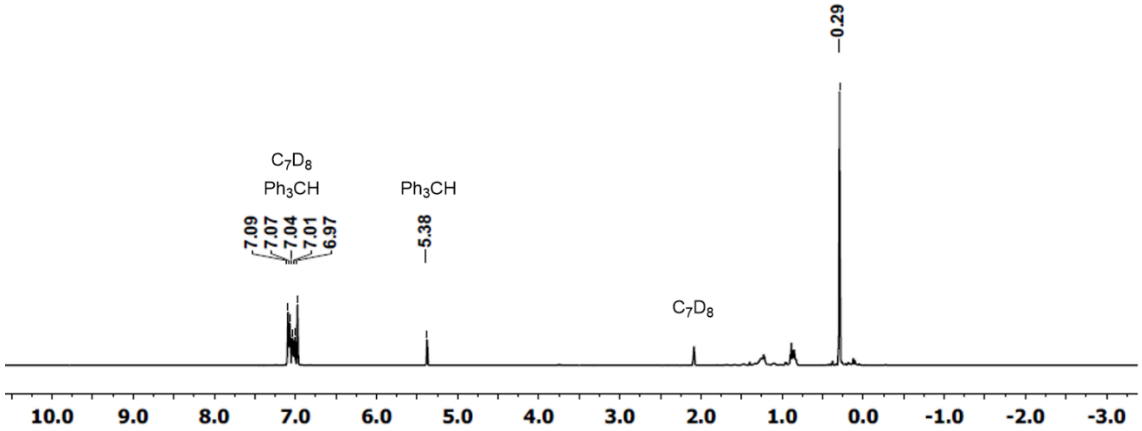

Figure S18a. ^{1}H NMR spectrum obtained from the non-polar phase of the reaction of silane **15** with $[Ph_3C][B(C_6F_5)_4]$.

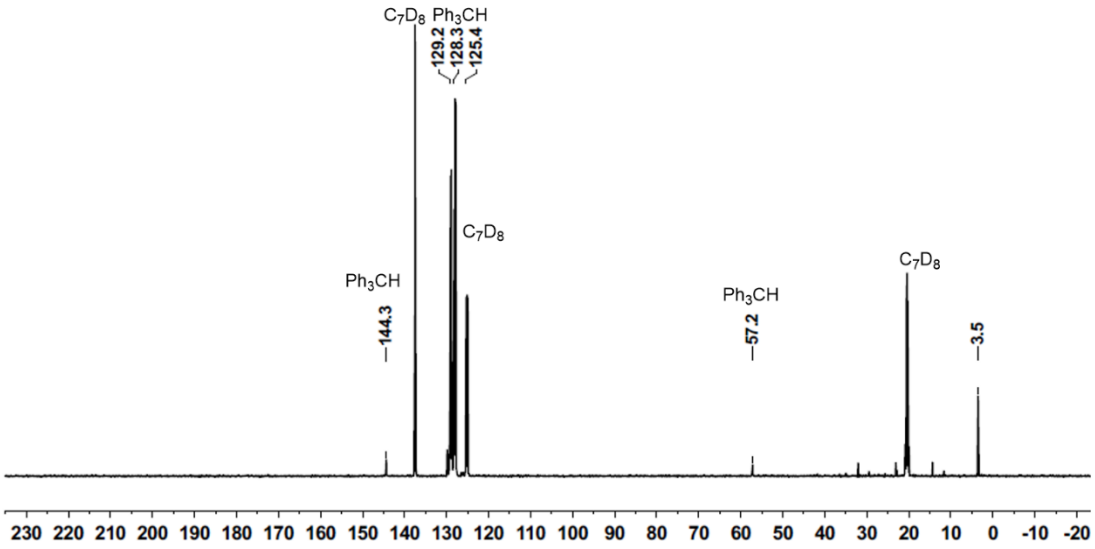

Figure S18b. $^{13}C\{^{1}H\}$ NMR spectrum obtained from the non-polar phase of the reaction of silane **15** with $[Ph_3C][B(C_6F_5)_4]$.

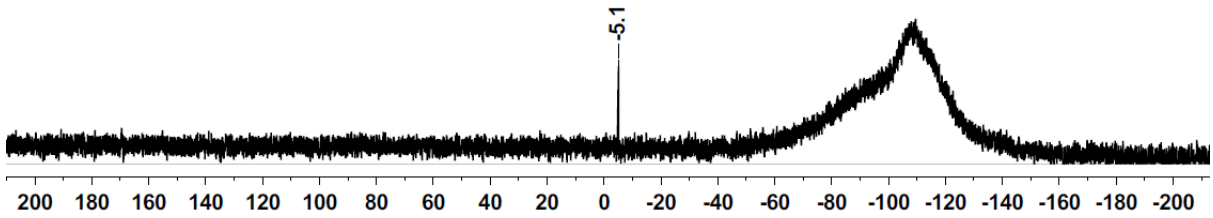

Figure S18c. $^{29}Si\{^{1}H\}$ NMR spectrum obtained from the non-polar phase of the reaction of silane **15** with $[Ph_3C][B(C_6F_5)_4]$.

Tris(trimethylsilyl)germyldimethylsilyl-phenylchloronium borate (8(C_6D_5Cl)[$B(C_6F_5)_4$]) from silane 15

0.09 g (0.25 mmol) tris(trimethylsilyl)germyldimethylsilane **15** and 0.23 g (0.25 mmol) triphenylmethyl tetrakis(pentafluorophenyl)borate were both dissolved in 0.5 mL chlorobenzene-d_5 and cooled to -20 °C. Germylsilane **15** was slowly added to the borate salt via a Teflon tube and the mixture was stirred at -20 °C for 1.5 h. The brown solution was transferred into a NMR tube at -20 °C and stored at -60 °C overnight until the NMR spectra were recorded the next morning. The mixture contained borate [**8**(C_6D_5Cl)][$B(C_6F_5)_4$], the rearrangement product **2** and triphenylmethane.

$^{29}Si\{^{1}H\}$ NMR (99.31 MHz, 253.0 K, C_6D_6Cl, δ ppm): -5.1 ($((CH_3)_3Si)_4Ge$), -1.4 ($(((CH_3)_3\underline{Si})_3GeSi(CH_3)_2^+$), 154.3 ($(((CH_3)_3Si)_3Ge\underline{Si}(CH_3)_2^+$).

Tris(trimethylsilyl)germyldimethylsilyl toluenium borate (8(C_7D_8)[$B(C_6F_5)_4$]) from germane 16

0.11 g (0.32 mmol) Bis(trimethylsilyl)pentamethyldisilanylgermane **16** and 0.29 g (0.32 mmol) triphenylmethyl tetrakis(pentafluorophenyl)borate were both dissolved in 1 mL toluene-d_8 and cooled to -20 °C.

Silylgermane **18** was slowly added to the borate salt via a Teflon tube and the mixture was stirred at -20 °C for 5 min. The brown polar phase and the light yellow non-polar phase were each transferred to separate NMR tubes at -20 °C and stored at -60 °C for 5 h until the NMR spectra were recorded. At -60°C the polar phase solidifies and no further reaction is expected. The NMR spectra of the polar phase recorded at -20°C contained nearly exclusively borate [**8**(C_7D_8)][$B(C_6F_5)_4$] (see Figure S12). The non-polar phase contained triphenylmethane and the rearrangement product **2**.

Polar phase:

^{1}H NMR (499.87 MHz, 253.0 K, C_7D_8, δ ppm): -0.16 (((CH$_3$)$_3$Si)$_3$GeSi(C<u>H</u>$_3$)$_2^+$), 0.12 (((C<u>H</u>$_3$)$_3$Si)$_3$GeSi(CH$_3$)$_2^+$). ^{13}C{^{1}H} NMR (125.71 MHz, 253.0 K, C_7D_8, δ ppm): 2.5 (((<u>C</u>H$_3$)$_3$Si)$_3$GeSi(CH$_3$)$_2^+$), 5.5 (((CH$_3$)$_3$Si)$_3$GeSi(<u>C</u>H$_3$)$_2^+$). ^{29}Si{^{1}H} NMR (99.31 MHz, 253.0 K, C_7D_8, δ ppm): -2.4 (((CH$_3$)$_3$<u>Si</u>)$_3$GeSi(CH$_3$)$_2^+$)), 98.2 (((CH$_3$)$_3$Si)$_3$Ge<u>Si</u>(CH$_3$)$_2^+$)).

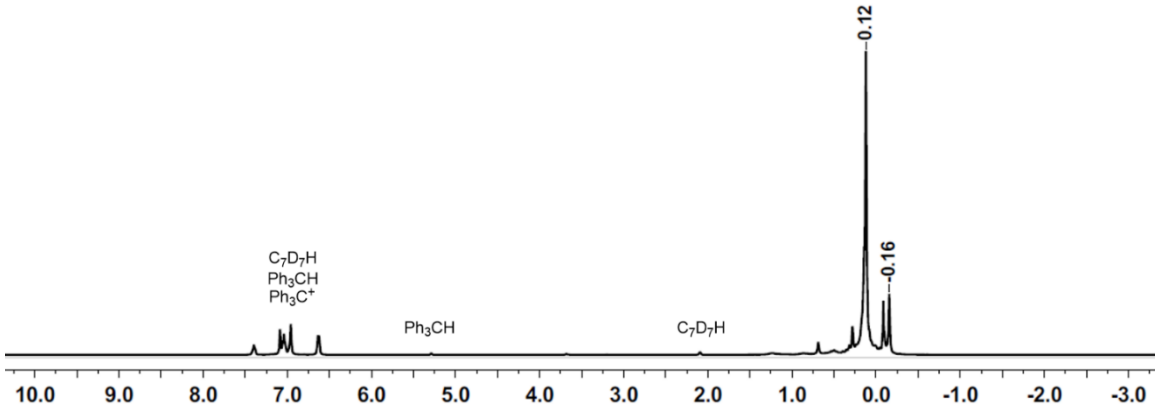

Figure S19a. ^{1}H NMR spectrum obtained from the polar phase of the reaction of germane **16** with [Ph_3C][$B(C_6F_5)_4$] after 5 min at -20°C.

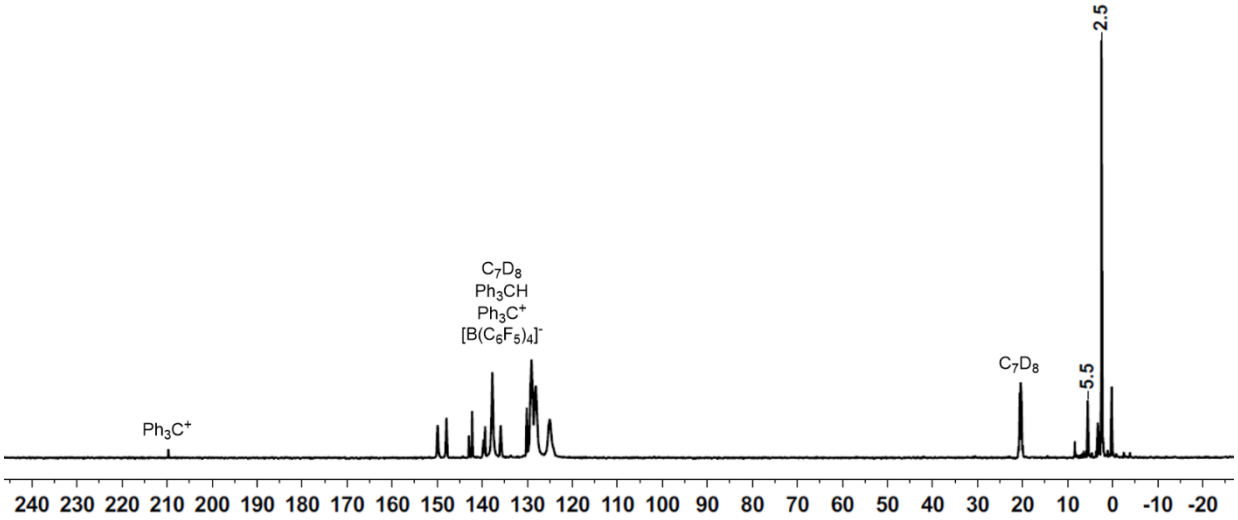

Figure S19b. ^{13}C{^{1}H} NMR spectrum obtained from the polar phase of the reaction of germane **16** with [Ph_3C][$B(C_6F_5)_4$] after 5 min at -20°C.

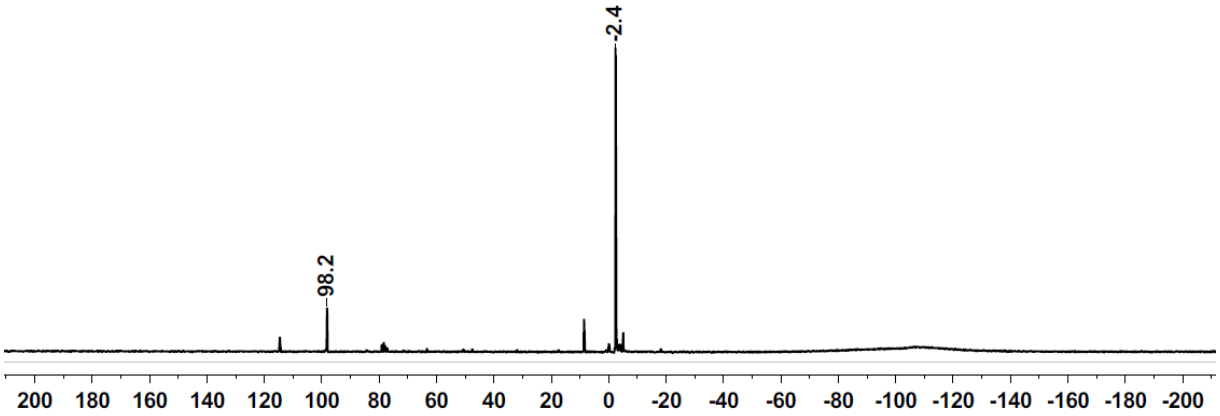

Figure S19c. $^{29}Si\{^{1}H\}$ NMR spectrum obtained from the polar phase of the reaction of germane **16** with $[Ph_3C][B(C_6F_5)_4]$ after 5 min at -20°C.

Non-polar phase:

^{1}H NMR (499.87 MHz, 305.0 K, C_7D_8, δ ppm): 0.30 (s, $((CH_3)_3Si)_4Ge$), 5.38 (s, $Ph_3\underline{C}H$), 6.98-7.10 (m, $\underline{Ph}_3CH$). $^{13}C\{^{1}H\}$ NMR (125.69 MHz, 305.0 K, C_7D_8, δ ppm): 3.5 $((CH_3)_3Si)_4Ge$), 57.1 ($Ph_3\underline{C}H$), 125.4 ($\underline{Ph}_3CH$), 128.2 ($\underline{Ph}_3CH$), 129.1 ($\underline{Ph}_3CH$), 144.3 ($\underline{Ph}_3CH$). $^{29}Si\{^{1}H\}$ NMR (99.31 MHz, 305.0 K, C_7D_8, δ ppm): -5.1 ($((CH_3)_3Si)_4Ge$).

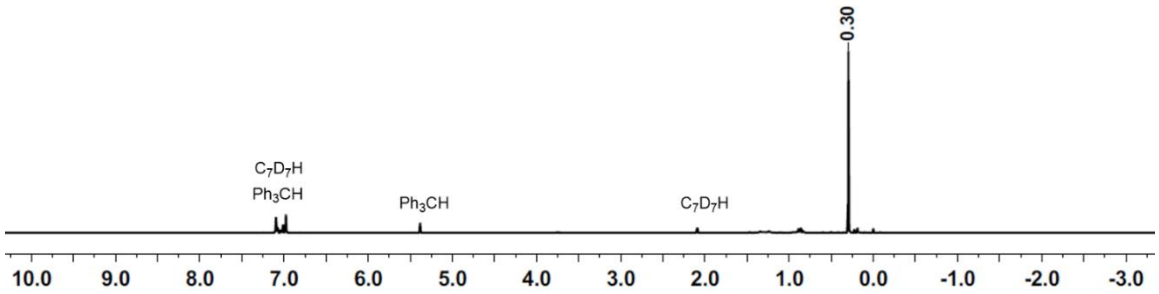

Figure S20a. ^{1}H NMR spectrum obtained from the non-polar phase of the reaction of germane **16** with $[Ph_3C][B(C_6F_5)_4]$.

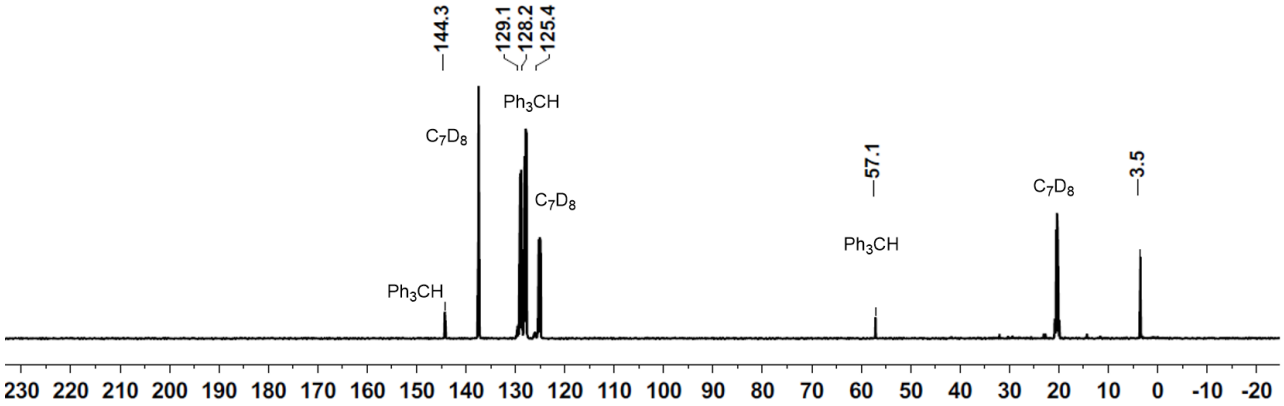

Figure S20b. ^{1}H NMR spectrum obtained from the non-polar phase of the reaction of germane **16** with $[Ph_3C][B(C_6F_5)_4]$.

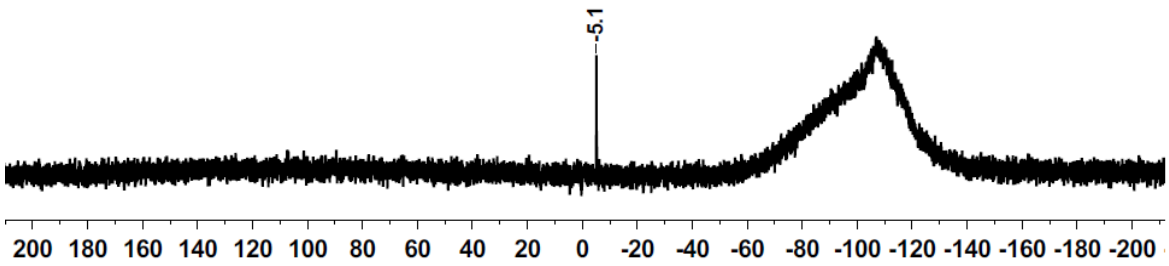

Figure S20c. $^{29}Si\{^{1}H\}$ NMR spectrum obtained from the non-polar phase of the reaction of germane **16** with $[Ph_3C][B(C_6F_5)_4]$.

Decomposition of silyl toluenium ion 8(C_7D_8) at higher temperatures

The thermolability of silyl toluenium ion **8**(C_7D_8) is shown by $^{29}Si\{^1H\}$ NMR spectroscopy at different temperatures. The amount of decomposition products increases with higher temperatures (Figure S14, b)-f)) and the intensity of **8**(C_7D_8) decreases. In the independent synthesis of **8**(C_7D_8) the same decomposition products already appear at -20 °C (Figure S14, a)).

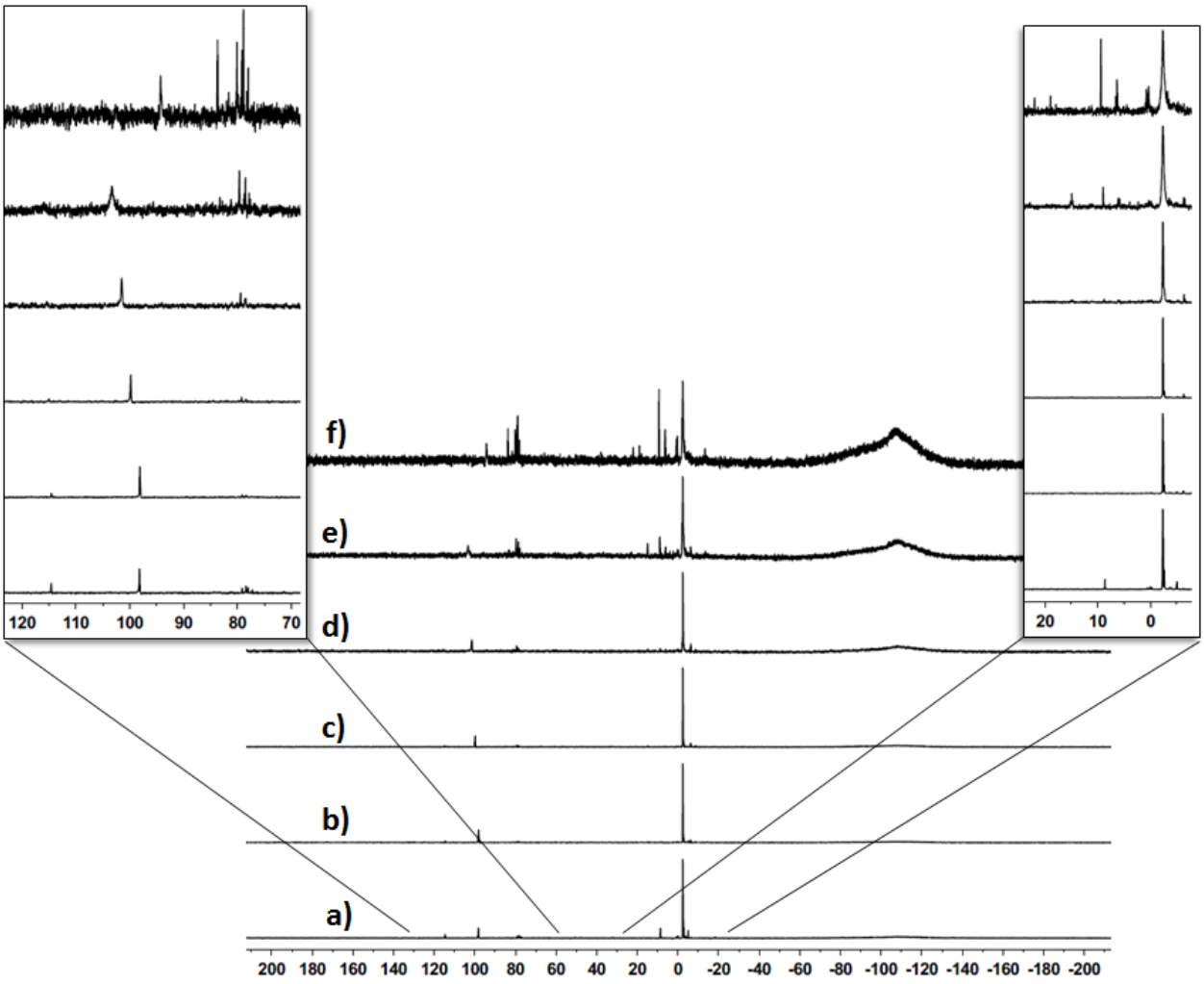

Figure S21. a) 99 MHz $^{29}Si\{^1H\}$ NMR spectrum (toluene-d_8, -20 °C) of silyl toluenium ion **8**(C_7D_8) at -20 °C in toluene synthesized by hydride transfer from germane **16** at -20 °. b-f) 99 MHz $^{29}Si\{^1H\}$ NMR spectra (toluene-d_8, -20 °C) of silyl toluenium ion **8**(C_7D_8) in toluene synthesized by hydride transfer from silane **15**. b) at -20°C c) at -10 °C; d) at 0 °C; **e**) at 10 °C, f) at 20 °C.

Computational Details

All quantum chemical calculations were carried out using the Gaussian09 package.[13] In order to be consistent with previously reported data[14], the molecular structures of toluene complexes [**3**(C_7H_8)]$^+$ - [**8**(C_7H_8)]$^+$ were optimized at the density functional B3LYP level of theory[15] using the 6-311+G(d,p) basis. Every stationary point was identified by a subsequent frequency calculation as minimum (Number of imaginary frequencies (NIMAG): 0). The SCF energies, E(SCF), for all optimized molecular structures obtained with this method are given in along with the corresponding Gibbs free energies at T=298.15K and p=0.101 MPa (1 atm) in the gas phase, G^{298}, are given in Table S1 and the Diagram of relative ground state energies E and Gibbs free energies at 298.15 K, G^{298}, of toluene complexes of isomeric cations **3** – **8** is given in Figure S22. The corresponding computed molecular structures are given in the form of their Cartesian coordinates in Table S2. NMR chemical shift computations were performed using the GIAO method as implemented in Gaussian 09 and the M06-L functional along with the 6-311G(2d,p) basis set for molecular structures obtained at the M06-2X/6-311+G(d,p) level of theory.[16] The influence of the highly polar medium on the structure optimizations was modeled using the PCM model[17] with a dielectric constant of 78.4.

Table S1. Absolute SCF energies (E(SCF) and free Gibbs enthalpies, G^{298}, for compounds of interest (at B3LYP/6-311+G(d,p)).

Compound	PG	E(SCF) [H/particle]	G^{298} [H/particle]	NIMAG
[**3**(C_7H_8)]$^+$	C1	-3945.83349	-3945.36640	0
[**4**(C_7H_8)]$^+$	C1	-3945.82084	-3945.35656	0
[**5**(C_7H_8)]$^+$	C1	-3945.83612	-3945.37290	0
[**6**(C_7H_8)]$^+$	C1	-3945.82962	-3945.36412	0
[**7**(C_7H_8)]$^+$	C1	-3945.84438	-3945.37829	0
[**8**(C_7H_8)]$^+$	C1	-3945.85031	-3945.38359	0

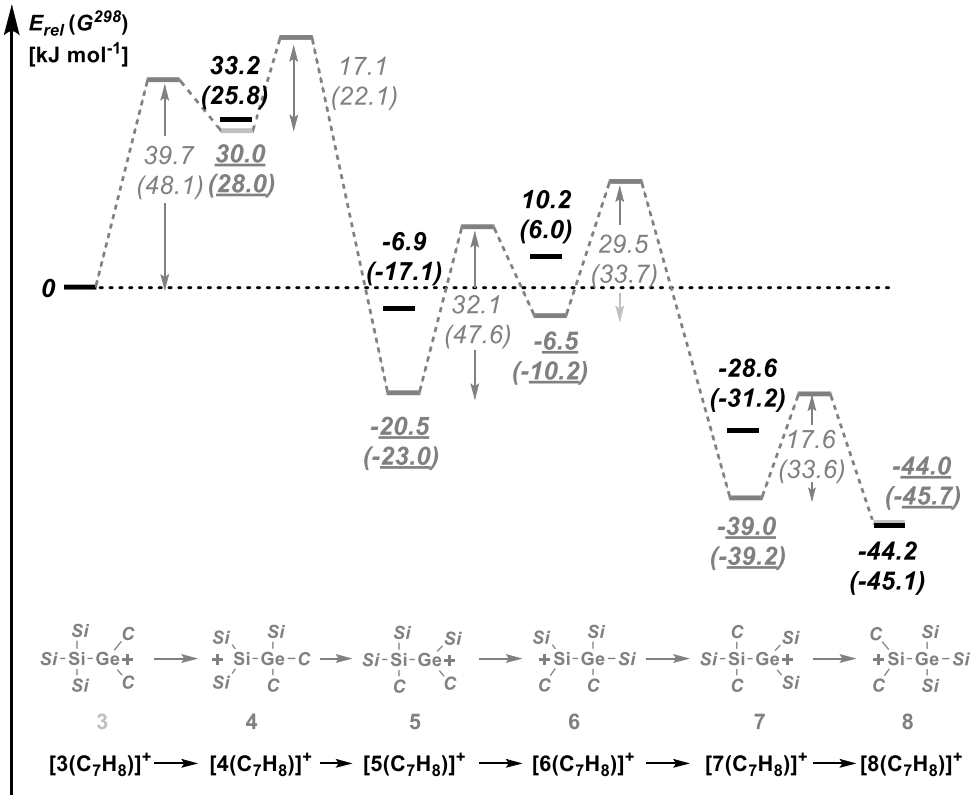

Figure S22. Diagram of relative ground state energies E and Gibbs free energies at 298.15 K, G^{298} (in parentheses), of toluene complexes of isomeric cations **3 – 8** (relative to cation [**3**$(C_7H_8)]^+$, calculated at B3LYP/6-311+G(d,p), in black). The complete reaction diagram for the isomerization of cations **3** → **8** as previously computed at B3LYP/6-311+G(d,p) is displayed in grey (from ref. 14, *Si* ≡ $SiMe_3$; *C* ≡ CH_3).

Table S2. Calculated molecular structures at B3LYP/6-311+G(d,p) in the form of their Cartesian coordinates.

Compound **[3(C_7H_8)]$^+$**

Standard orientation:

Center Number	Atomic Number	Atomic Type	Coordinates (Angstroms) X	Y	Z
1	14	0	1.221865	0.123391	0.070805
2	14	0	1.081128	2.500044	0.385119
3	14	0	2.113682	-1.060703	1.960967
4	14	0	2.459659	-0.373862	-1.954384
5	6	0	0.561165	2.910511	2.159080
6	1	0	0.475922	3.996924	2.269067
7	1	0	-0.400318	2.478490	2.447894
8	1	0	1.304899	2.570195	2.884272
9	6	0	-0.136722	3.281153	-0.835253
10	1	0	-1.162543	2.932333	-0.691650
11	1	0	-0.139232	4.367791	-0.698224
12	1	0	0.143867	3.083862	-1.872918
13	6	0	2.801788	3.223889	0.088910
14	1	0	3.134306	3.096227	-0.944110
15	1	0	2.779816	4.299454	0.294410
16	1	0	3.556080	2.781571	0.744461
17	6	0	3.615384	-0.098154	2.585329
18	1	0	3.347277	0.897718	2.947320
19	1	0	4.069458	-0.638763	3.422562
20	1	0	4.382351	0.016911	1.815309
21	6	0	4.293003	-0.179540	-1.537407
22	1	0	4.629685	-0.910745	-0.798470
23	1	0	4.883214	-0.336836	-2.446793
24	1	0	4.529090	0.818141	-1.160370
25	6	0	0.825111	-1.173948	3.345284
26	1	0	1.287784	-1.612012	4.236005
27	1	0	0.432112	-0.195050	3.632604
28	1	0	-0.016089	-1.819671	3.075649
29	6	0	2.644895	-2.809994	1.477754
30	1	0	3.042790	-3.322721	2.360076
31	1	0	1.816197	-3.413292	1.097763
32	1	0	3.434296	-2.807282	0.721883
33	6	0	2.144009	-2.140184	-2.556886
34	1	0	2.818200	-2.355842	-3.392703
35	1	0	2.336004	-2.887842	-1.783292
36	1	0	1.124906	-2.283486	-2.927746
37	6	0	1.990802	0.831197	-3.333784
38	1	0	2.561545	0.584293	-4.235520
39	1	0	0.930615	0.779204	-3.595715
40	1	0	2.223980	1.867198	-3.076096
41	32	0	-0.893106	-0.878612	-0.542977

42	6	0	-1.894130	-0.253010	-2.111987
43	1	0	-2.942198	-0.547429	-2.041944
44	1	0	-1.820407	0.825663	-2.237373
45	1	0	-1.459956	-0.745240	-2.987849
46	6	0	-1.017018	-2.842921	-0.416567
47	1	0	-0.873371	-3.193627	0.605672
48	1	0	-1.973056	-3.200997	-0.798669
49	1	0	-0.213488	-3.257067	-1.031446
50	6	0	-4.989005	0.326774	0.004151
51	6	0	-4.041323	1.308311	0.338077
52	6	0	-2.866511	0.971267	0.991243
53	6	0	-2.585175	-0.374883	1.311134
54	6	0	-3.552453	-1.356815	1.007863
55	6	0	-4.722655	-1.008755	0.351438
56	1	0	-4.245895	2.347038	0.103287
57	1	0	-2.169531	1.747725	1.280128
58	1	0	-1.784137	-0.605721	2.006145
59	1	0	-3.388777	-2.384980	1.307264
60	1	0	-5.458819	-1.772668	0.127263
61	6	0	-6.259376	0.698569	-0.708607
62	1	0	-6.612585	1.685261	-0.402930
63	1	0	-6.092942	0.734513	-1.791091
64	1	0	-7.051062	-0.028649	-0.522587

Compound **[4(C_7H_8)]$^+$**

Standard orientation:

Center Number	Atomic Number	Atomic Type	Coordinates (Angstroms) X	Y	Z
1	14	0	-0.362778	0.379834	0.041261
2	14	0	-0.496110	2.787683	0.150304
3	14	0	-0.986991	-0.770080	2.059852
4	32	0	1.681838	-0.424522	-1.084065
5	14	0	3.667820	-0.651172	0.332827
6	6	0	2.059985	0.806717	-2.603184
7	1	0	2.905986	0.406210	-3.166815
8	1	0	1.210627	0.880866	-3.286343
9	1	0	2.323546	1.808699	-2.261624
10	6	0	1.362272	-2.213013	-1.906630
11	1	0	2.321402	-2.606336	-2.251330
12	1	0	0.940319	-2.925439	-1.196350
13	1	0	0.709007	-2.136822	-2.778441
14	6	0	4.061145	0.897533	1.336350
15	1	0	3.285354	1.140685	2.065946
16	1	0	4.992166	0.737586	1.890722
17	1	0	4.210953	1.771700	0.697507
18	6	0	5.068531	-0.978863	-0.893360

19	1	0	5.227255	-0.134845	-1.569690
20	1	0	6.002605	-1.139061	-0.344072
21	1	0	4.890642	-1.870571	-1.500260
22	6	0	3.458602	-2.142701	1.473481
23	1	0	4.392353	-2.320939	2.017222
24	1	0	2.672112	-1.995666	2.217716
25	1	0	3.229516	-3.053158	0.912985
26	6	0	0.184168	-0.058262	3.366885
27	1	0	0.000811	1.003993	3.548481
28	1	0	0.011178	-0.583410	4.312727
29	1	0	1.239746	-0.183868	3.116172
30	6	0	-0.716471	-2.630148	1.891988
31	1	0	-1.382837	-3.078202	1.151147
32	1	0	0.312067	-2.877552	1.619142
33	1	0	-0.924916	-3.112280	2.853133
34	6	0	-2.766079	-0.418396	2.582463
35	1	0	-2.948448	-0.899526	3.549540
36	1	0	-2.961412	0.649297	2.704660
37	1	0	-3.493427	-0.816576	1.873290
38	6	0	-0.588884	3.547385	-1.578446
39	1	0	-1.511941	3.312695	-2.114185
40	1	0	-0.545211	4.637640	-1.482308
41	1	0	0.250861	3.241936	-2.206302
42	6	0	1.096575	3.359058	0.990556
43	1	0	1.219052	2.939760	1.991898
44	1	0	1.986855	3.113517	0.407757
45	1	0	1.063314	4.448965	1.096064
46	6	0	-1.975714	3.332730	1.190177
47	1	0	-2.015544	4.427114	1.211111
48	1	0	-2.932076	2.978206	0.798983
49	1	0	-1.888614	2.991225	2.224852
50	6	0	-3.087413	0.740219	-1.346017
51	6	0	-4.272247	0.177552	-0.905244
52	6	0	-4.413344	-1.216089	-0.797436
53	6	0	-3.314704	-2.032153	-1.122273
54	6	0	-2.124172	-1.482895	-1.561293
55	6	0	-1.970407	-0.075098	-1.656567
56	1	0	-3.023036	1.811471	-1.484046
57	1	0	-5.115810	0.816752	-0.671318
58	1	0	-3.415868	-3.110038	-1.058563
59	1	0	-1.308483	-2.130095	-1.853974
60	1	0	-1.198978	0.326568	-2.309263
61	6	0	-5.713453	-1.832623	-0.367413
62	1	0	-6.116808	-2.464689	-1.164759

63	1	0	-5.570685	-2.476683	0.505375
64	1	0	-6.459958	-1.077859	-0.120334

Compound **[5(C_7H_8)]$^+$**

Standard orientation:

Center Number	Atomic Number	Atomic Type	Coordinates (Angstroms) X	Y	Z
1	32	0	-0.437747	0.256388	-0.565651
2	14	0	-1.848288	2.242630	-0.180697
3	14	0	1.635615	-0.288111	0.619093
4	14	0	2.638387	-2.310976	-0.191730
5	14	0	3.059020	1.622235	0.286335
6	6	0	-0.321171	-0.160268	-2.499527
7	1	0	0.015837	-1.181907	-2.677224
8	1	0	-1.269576	0.008859	-3.009142
9	1	0	0.426559	0.518537	-2.922752
10	6	0	-0.879410	3.638479	-1.008291
11	1	0	-1.455210	4.564911	-0.902064
12	1	0	0.099257	3.812613	-0.557124
13	1	0	-0.739851	3.466169	-2.078762
14	6	0	-3.505176	2.039596	-1.050297
15	1	0	-4.051714	2.987536	-0.996367
16	1	0	-3.383437	1.792401	-2.108042
17	1	0	-4.124984	1.270218	-0.588627
18	6	0	-2.046318	2.556331	1.663991
19	1	0	-2.606175	1.758995	2.157722
20	1	0	-1.081966	2.658591	2.168204
21	1	0	-2.596845	3.490517	1.817644
22	6	0	3.415206	-2.028022	-1.891994
23	1	0	3.858316	-2.962450	-2.252066
24	1	0	2.683715	-1.706610	-2.638407
25	1	0	4.213613	-1.281953	-1.862826
26	6	0	1.386410	-3.729144	-0.319622
27	1	0	1.923639	-4.653577	-0.557201
28	1	0	0.850038	-3.904540	0.617261
29	1	0	0.653424	-3.577191	-1.117260
30	6	0	3.966914	-2.797588	1.062621
31	1	0	3.543892	-2.987850	2.052877
32	1	0	4.459140	-3.719181	0.734264
33	1	0	4.739091	-2.031769	1.167373
34	6	0	4.817318	1.098626	0.745053
35	1	0	5.217240	0.344474	0.062807
36	1	0	5.477212	1.971323	0.692810
37	1	0	4.878794	0.703644	1.762538
38	6	0	3.032407	2.213809	-1.510666
39	1	0	2.066319	2.633036	-1.805392
40	1	0	3.778802	3.003706	-1.645044

41	1	0	3.281673	1.410703	-2.209695
42	6	0	2.514858	3.010462	1.450232
43	1	0	2.587000	2.705058	2.497662
44	1	0	3.167599	3.879930	1.318813
45	1	0	1.489274	3.341152	1.268800
46	6	0	1.239504	-0.438181	2.482949
47	1	0	0.687779	-1.352554	2.715594
48	1	0	2.175254	-0.478621	3.048064
49	1	0	0.668346	0.414786	2.857132
50	6	0	-4.127913	-1.700340	-0.758579
51	6	0	-2.780187	-1.940897	-0.969494
52	6	0	-1.858821	-1.802852	0.089568
53	6	0	-2.336877	-1.437626	1.364941
54	6	0	-3.688961	-1.195857	1.562353
55	6	0	-4.608446	-1.336690	0.511622
56	1	0	-4.828120	-1.816425	-1.578513
57	1	0	-2.436945	-2.263831	-1.945180
58	1	0	-0.868012	-2.233386	-0.006983
59	1	0	-1.650505	-1.372303	2.200598
60	1	0	-4.046576	-0.922904	2.548969
61	6	0	-6.081473	-1.140389	0.742669
62	1	0	-6.557902	-0.644553	-0.105910
63	1	0	-6.573801	-2.111249	0.865890
64	1	0	-6.275716	-0.556298	1.643208

Compound **[6(C_7H_8)]$^+$**

Standard orientation:

Center Number	Atomic Number	Atomic Type	Coordinates (Angstroms) X	Y	Z
1	32	0	-0.966844	-0.346516	-0.387148
2	14	0	-1.887664	-2.306926	0.761038
3	14	0	-2.744755	1.343867	-0.644339
4	14	0	0.841495	0.794968	0.785910
5	14	0	1.664333	2.980807	0.175295
6	6	0	3.354066	3.250872	0.982275
7	1	0	3.656761	4.290693	0.818022
8	1	0	3.332007	3.094217	2.064580
9	1	0	4.142831	2.622095	0.560944
10	6	0	0.438100	4.219541	0.905164
11	1	0	-0.557778	4.142482	0.465046
12	1	0	0.342411	4.114224	1.989079
13	1	0	0.804030	5.232914	0.707796
14	6	0	1.793333	3.188835	-1.695293
15	1	0	2.560164	2.549736	-2.139866
16	1	0	0.849446	2.979119	-2.202902
17	1	0	2.065125	4.224602	-1.924422
18	6	0	0.610356	0.742968	2.665259

19	1	0	0.418900	-0.262049	3.045496
20	1	0	1.450422	1.174702	3.214793
21	1	0	-0.274192	1.348288	2.896815
22	6	0	-3.144539	2.180728	1.003225
23	1	0	-3.466062	1.457739	1.757303
24	1	0	-2.298372	2.738562	1.412376
25	1	0	-3.964812	2.892810	0.863458
26	6	0	-2.246274	2.629503	-1.937209
27	1	0	-1.991960	2.164780	-2.893777
28	1	0	-3.087268	3.307702	-2.117366
29	1	0	-1.397745	3.239426	-1.621179
30	6	0	-4.281299	0.437010	-1.270889
31	1	0	-5.072558	1.170561	-1.461228
32	1	0	-4.096956	-0.093274	-2.208852
33	1	0	-4.670263	-0.280136	-0.544317
34	6	0	-0.573313	-3.506433	1.401459
35	1	0	0.058729	-3.889027	0.596721
36	1	0	0.070684	-3.055886	2.160598
37	1	0	-1.073461	-4.364466	1.863562
38	6	0	-2.946993	-3.209936	-0.517084
39	1	0	-3.416460	-4.083742	-0.052569
40	1	0	-3.745164	-2.580613	-0.916649
41	1	0	-2.348541	-3.568000	-1.359345
42	6	0	-2.951141	-1.744613	2.219649
43	1	0	-3.795054	-1.125071	1.906163
44	1	0	-3.364552	-2.622418	2.727577
45	1	0	-2.377169	-1.180542	2.960205
46	6	0	2.958029	-0.315351	0.717066
47	6	0	2.737720	-1.584702	1.300528
48	6	0	3.313542	-0.254922	-0.653916
49	6	0	2.809076	-2.731660	0.528888
50	1	0	2.538973	-1.658356	2.363041
51	6	0	3.370118	-1.406580	-1.415838
52	1	0	3.563490	0.698576	-1.102198
53	6	0	3.126428	-2.665512	-0.837902
54	1	0	2.646951	-3.698565	0.989926
55	1	0	3.640128	-1.345345	-2.464092
56	6	0	3.203698	-3.912977	-1.670766
57	1	0	3.371534	-4.798102	-1.055888
58	1	0	2.265310	-4.062357	-2.217358
59	1	0	4.000516	-3.845465	-2.414200
60	6	0	-0.338554	-0.817331	-2.225191
61	1	0	0.077080	0.053647	-2.733488
62	1	0	0.418516	-1.600569	-2.192655
63	1	0	-1.188176	-1.182175	-2.805434
64	1	0	3.229692	0.513159	1.365804

Compound **[7(C$_7$H$_8$)]$^+$**

Standard orientation:

Center Number	Atomic Number	Atomic Type	Coordinates (Angstroms) X	Y	Z
1	32	0	-0.176376	0.460499	0.226521
2	14	0	-1.997492	0.830170	1.852293
3	14	0	0.211872	2.341948	-1.327374
4	14	0	1.853411	-0.629627	1.139415
5	14	0	3.643090	-1.074685	-0.378646
6	6	0	4.840062	-2.197351	0.562735
7	1	0	5.701755	-2.431939	-0.071000
8	1	0	5.223202	-1.720832	1.469432
9	1	0	4.376707	-3.144763	0.850873
10	6	0	4.531571	0.525539	-0.854412
11	1	0	3.909366	1.198993	-1.449377
12	1	0	4.869427	1.073382	0.029706
13	1	0	5.419129	0.291717	-1.451365
14	6	0	3.035717	-1.972947	-1.931338
15	1	0	2.488506	-2.888755	-1.689496
16	1	0	2.393841	-1.344576	-2.555401
17	1	0	3.892702	-2.264044	-2.547477
18	6	0	1.386060	-2.235458	2.045044
19	1	0	2.203958	-2.496675	2.724612
20	1	0	0.479486	-2.139179	2.646247
21	1	0	1.258162	-3.081672	1.365516
22	6	0	2.403462	0.641154	2.449352
23	1	0	1.665954	0.759927	3.247521
24	1	0	3.326564	0.281373	2.916013
25	1	0	2.615337	1.626380	2.028139
26	6	0	1.403764	3.473975	-0.396672
27	1	0	0.988888	3.825494	0.551532
28	1	0	2.360053	2.987442	-0.191944
29	1	0	1.608792	4.358221	-1.009977
30	6	0	0.992172	1.752065	-2.941444
31	1	0	0.324297	1.122723	-3.535011
32	1	0	1.236488	2.626036	-3.555023
33	1	0	1.920468	1.200784	-2.778019
34	6	0	-1.403322	3.252543	-1.675592
35	1	0	-1.210759	4.072549	-2.375806
36	1	0	-2.164017	2.609655	-2.124677
37	1	0	-1.825853	3.691783	-0.768385
38	6	0	-2.178200	-0.630101	3.029525
39	1	0	-2.447242	-1.552274	2.509908
40	1	0	-1.263755	-0.812168	3.598873
41	1	0	-2.974002	-0.412873	3.750231
42	6	0	-3.638019	1.210658	1.006196
43	1	0	-4.381831	1.453714	1.772953

44	1	0	-3.567281	2.066515	0.331367
45	1	0	-4.014227	0.359603	0.436459
46	6	0	-1.399466	2.356660	2.797426
47	1	0	-1.322644	3.239724	2.157717
48	1	0	-2.128141	2.587594	3.582606
49	1	0	-0.434159	2.204217	3.285919
50	6	0	-2.565977	-2.704452	-0.412609
51	6	0	-3.598067	-2.099130	-1.142470
52	6	0	-3.272581	-1.058034	-2.032566
53	6	0	-1.962677	-0.649019	-2.202146
54	6	0	-0.920225	-1.259594	-1.466273
55	6	0	-1.245633	-2.308515	-0.579863
56	1	0	-2.798641	-3.518997	0.263936
57	1	0	-4.059954	-0.591364	-2.614311
58	1	0	-1.729283	0.117263	-2.930860
59	1	0	0.105934	-1.139956	-1.799409
60	1	0	-0.458277	-2.830069	-0.051509
61	6	0	-5.024233	-2.548660	-0.990116
62	1	0	-5.613550	-1.791092	-0.462299
63	1	0	-5.493868	-2.694346	-1.966158
64	1	0	-5.096297	-3.480781	-0.429049

Compound **[8(C_7H_8)]$^+$**

Standard orientation:

Center Number	Atomic Number	Atomic Type	Coordinates (Angstroms) X	Y	Z
1	14	0	-1.101836	-0.842263	0.743822
2	32	0	1.007149	0.045591	-0.029523
3	14	0	0.876315	2.356584	-0.829667
4	14	0	1.923106	-1.492105	-1.704257
5	14	0	2.334516	-0.031004	2.053026
6	6	0	-1.116456	-2.708034	1.005521
7	1	0	-0.298169	-2.952420	1.691007
8	1	0	-2.046837	-3.056040	1.459434
9	1	0	-0.940144	-3.267088	0.084160
10	6	0	-1.980805	0.016857	2.161495
11	1	0	-1.932044	1.103824	2.091672
12	1	0	-3.027040	-0.288556	2.241820
13	1	0	-1.483820	-0.285759	3.090424
14	6	0	0.621738	-1.893890	-3.021543
15	1	0	0.212431	-0.994618	-3.489957
16	1	0	1.078959	-2.493074	-3.816313
17	1	0	-0.207930	-2.483406	-2.619672
18	6	0	2.613001	3.095214	-0.740935
19	1	0	2.595552	4.113380	-1.144561
20	1	0	2.986337	3.157936	0.284275
21	1	0	3.333704	2.522088	-1.329964

22	6	0	3.399291	-0.648298	-2.527058
23	1	0	3.856192	-1.333544	-3.249108
24	1	0	3.110730	0.254560	-3.071582
25	1	0	4.170672	-0.373405	-1.803226
26	6	0	2.492822	-3.100122	-0.889535
27	1	0	1.676884	-3.630520	-0.392024
28	1	0	2.903219	-3.771658	-1.651365
29	1	0	3.279857	-2.927344	-0.150903
30	6	0	-0.290601	3.390776	0.243815
31	1	0	-0.291669	4.426697	-0.111967
32	1	0	-1.324118	3.035801	0.216243
33	1	0	0.029568	3.404721	1.288735
34	6	0	0.306712	2.402326	-2.635656
35	1	0	0.236998	3.443014	-2.970092
36	1	0	1.023112	1.899171	-3.290524
37	1	0	-0.669606	1.940255	-2.803343
38	6	0	2.066472	-1.646996	3.001492
39	1	0	2.258927	-2.529118	2.385517
40	1	0	2.762033	-1.682683	3.847062
41	1	0	1.058118	-1.731544	3.416750
42	6	0	1.873380	1.420114	3.172449
43	1	0	2.461187	1.368504	4.095368
44	1	0	2.085068	2.384998	2.705363
45	1	0	0.817754	1.407840	3.456631
46	6	0	4.152550	0.093733	1.554623
47	1	0	4.772716	0.116222	2.457371
48	1	0	4.474236	-0.763992	0.958649
49	1	0	4.366136	1.001238	0.985374
50	6	0	-2.986618	0.691628	-0.975931
51	6	0	-2.658586	-0.687247	-1.026311
52	6	0	-3.634637	-1.620724	-0.596336
53	6	0	-4.827774	-1.188383	-0.044175
54	6	0	-5.123928	0.182810	0.054273
55	6	0	-4.183817	1.111767	-0.426721
56	1	0	-2.293237	1.419932	-1.376170
57	1	0	-1.874025	-1.018351	-1.701235
58	1	0	-3.447078	-2.681628	-0.707957
59	1	0	-5.560056	-1.915384	0.288463
60	1	0	-4.415785	2.170203	-0.389084
61	6	0	-6.417747	0.647976	0.657862
62	1	0	-6.284376	0.848712	1.727133
63	1	0	-6.762713	1.574568	0.195537
64	1	0	-7.199905	-0.106473	0.561901

References

[1] (a) Massey, A. G.; Park, A. J. *J. Organomet. Chem.* **1964**, *2*, 245-250. (b) Chien, J. C. W.; Tsai, W. M.; Rausch, M. D. *J. Am. Chem. Soc.* **1991**, *113*, 8570-8571.

[2] Gilman, H.; Smith, C. L. *J. Organomet. Chem.* **1967**, *8*, 245-253.

[3] Brook, A. G.; Abdesaken, F.; Söllradl, H. *J. Organomet. Chem.* **1986**, *299*, 9-13.

[4] Marschner, C. *Eur. J. Inorg. Chem.* **1998**, *1998*, 221-226.

[5] Fischer, J.; Baumgartner, J.; Marschner, C. *Organometallics* **2005**, *24*, 1263-1268.

[6] Mallela, S. P.; Ghuman, M. A.; Geanangel, R. A. *Inorg. Chim. Acta* **1992**, *202*, 211-217.

[7] Gluyas, J. B. G.; Burschka, C.; Kraft, P.; Tacke, R. *Organometallics* **2010**, *29*, 5897-5903.

[8] Lehmann, M.; Schulz, A.; Villinger, A. *Angew. Chem. Int. Ed.* **2009**, *48*, 7444-7447.

[9] (a) West, R.; Hunt, H. R.; Whipple, R. O. *J. Am. Chem. Soc.* **1954**, *76*, 310-310. (b) Moedritzer, K.; Van Wazer, J. R. *Inorg. Chem.* **1965**, *4*, 1753-1760.

[10] Sharma, S.; Pannell, K. H. *Organometallics* **2000**, *19*, 1225.

[11] Schäfer, A.; Schäfer, A.; Müller, T. *Dalton Trans.* **2010**, *39*, 9296-9303.

[12] Baumgartner, J.; Fischer, R.; Fischer, J.; Wallner, A.; Marschner, C.; Flörke, U. *Organometallics* **2005**, *24*, 6450-6457.

[13] Frisch, M. J. T., G. W.; Cheeseman, J. R.; Scalmani, G.; Caricato, M.; Hratchian, H. P.; Li, X.; Barone, V.; Bloino, J.; Zheng, G.; Vreven, T.; Montgomery, J. A.; Petersson, G.; A.; Scuseria, G. E. S., H. B.; Nakatsuji, H.; Izmaylov, A. F.; Martin, R. L.;; Sonnenberg, J. L. P., J. E.; Heyd, J. J.; Brothers, E.; Ogliaro, F.; Bearpark, M.; Robb,; M. A.; Mennucci, B. K., K. N.; Staroverov, V. N.; Kobayashi, R.; Normand, J.;; Rendell, A. G., R.; Zakrzewski, V. G.; Hada, M.; Ehara, M.; Toyota, K.; Fukuda,; R.; Hasegawa, J. I., M.; Nakajima, T.; Honda, Y.; Kitao, O.; Nakai, H. *Gaussian 09*.

[14] Wagner, H.; Baumgartner, J.; Müller, T.; Marschner, C. *J. Am. Chem. Soc.* **2009**, *131*, 5022-5023.

[15] (a) Lee, C.; Yang, W.; Parr, R. G. *Phys. Rev. B* **1988**, *37*, 785-789. (b) Becke, A. D. *J. Chem. Phys.* **1993**, *98*, 5648-5652.

[16] Zhao, Y.; Truhlar, D. *Theor. Chem. Acc.* **2008**, *120*, 215-241.

[17] Tomasi, J.; Mennucci, B.; Cammi, R. *Chem. Rev.* **2005**, *105*, 2999-3094.